PLANETARY SCIENCE

Martian subsurface cryosalt expansion and collapse as trigger for landslides

J. L. Bishop[1,2]*, M. Yeşilbaş[1,3], N. W. Hinman[4], Z. F. M. Burton[5], P. A. J. Englert[6], J. D. Toner[7], A. S. McEwen[8], V. C. Gulick[1,2], E. K. Gibson[9], C. Koeberl[10]

On Mars, seasonal martian flow features known as recurring slope lineae (RSL) are prevalent on sun-facing slopes and are associated with salts. On Earth, subsurface interactions of gypsum with chlorides and oxychlorine salts wreak havoc: instigating sinkholes, cave collapse, debris flows, and upheave. Here, we illustrate (i) the disruptive potential of sulfate-chloride reactions in laboratory soil crust experiments, (ii) the formation of thin films of mixed ice-liquid water "slush" at −40° to −20°C on salty Mars analog grains, (iii) how mixtures of sulfates and chlorine salts affect their solubilities in low-temperature environments, and (iv) how these salt brines could be contributing to RSL formation on Mars. Our results demonstrate that interactions of sulfates and chlorine salts in fine-grained soils on Mars could absorb water, expand, deliquesce, cause subsidence, form crusts, disrupt surfaces, and ultimately produce landslides after dust loading on these unstable surfaces.

INTRODUCTION

Chemical alteration on Mars has largely taken place through reactions in liquid water. Although geologic features and mineralogy required liquid water on the martian surface, it may have been short-lived (*1*). Liquid water is not currently stable on the surface of Mars (*2*), and long-term liquid water is inconsistent with climate modeling (*3*). However, H_2O ice is present just below the surface at the Phoenix landing site (*4*) and at several other mid-latitude sites identified from orbit either in High-Resolution Imaging Science Experiment (HiRISE) images (*5*), or through analyses of Gamma Ray Spectrometer (GRS) data (*6*). Seasonal frost coatings on ice at scarps (Fig. 1, A and B) (*5*) confirm interactions of surface and atmospheric H_2O, and the recent slope failures and landslides in inverted terrains are consistent with terrestrial permafrost features, suggesting a substantial water ice component in some clay-rich sediments today (*7*). Recurring slope lineae (RSL) features are well documented across the equatorial regions and mid-latitudes of Mars (*8*), and multiple "wet" or "dry" formation processes have been proposed to explain these seasonally reappearing flows (*9*, *10*), although none of these mechanisms are fully consistent with the observed RSL. We propose a hybrid model that includes both wet and dry components of salty soils on Mars based on field observations, laboratory experiments, and modeling of brines.

Subsurface liquid water and salt in Antarctica

The McMurdo Dry Valleys (MDV) have long been investigated as analogs for Mars due to the cold and arid climate and scarcity of life (*11*). Permafrost depth here responds to climatic variability, producing salts and other minerals at multiple depths in the Antarctic sediments (*12*). Early work in the MDV demonstrated the presence of thin films of liquid water coating mineral grains in frozen soils (*13*). Despite limited liquid water availability and freezing conditions, migration of salts and water-soluble ions in the MDV has been documented (*14*). Investigation of multiple soil and sediment samples from Wright Valley confirmed concentration of salts and chemical weathering below the surface (*15*). Consistent with previous studies, we documented soil pits in Wright Valley, Antarctica containing (i) aeolian material in the upper 1 to 2 cm, (ii) a near-surface zone dominated by chemical alteration where sulfates and chlorides are concentrated and where thin films of liquid water can form, and (iii) a deeper, permanently frozen zone that contains stable ice and permafrost with little to no change in the concentrations of dissolved species. Chlorides and Ca sulfates are abundant in near-surface MDV soils and sediments that are above the permanently frozen line but contain ice during cold seasons [e.g., (*15*, *16*, *17*)] and could be contributing to the chemical activity of soils through the formation of thin films of brine water. Near-surface layers of bright materials are frequently dominated by halite (NaCl), $CaCl_2$, and/or gypsum ($CaSO_4{\cdot}2H_2O$) (Fig. 1, C to E). These salt-enriched layers contain a few weight % (wt %) chloride and gypsum or anhydrite and tend to be present 3 to 7 cm below the surface in evaporative settings including the margins of Don Juan Pond and Don Quixote Pond in Wright Valley. Despite this evidence of chemical alteration below the surface, alteration of surface materials in the MDV is dominated by physical alteration (*18*).

Notable physical alteration has occurred on Mars as well through impacts, wind abrasion, and other aeolian processes (*19*) over millions to billions of years, producing a substantial portion of surface fines <40 μm in diameter that are transported and deposited across the surface (*20*). Analyses of modern surface regolith by the Chemistry and Mineralogy (CheMin) X-ray diffraction (XRD) instrument on the Curiosity rover indicate that ~30 wt % of modern aeolian sediments contain nanophase, poorly crystalline, or amorphous phases (*21*). This abundant poorly crystalline and fine-grained material on Mars is likely highly susceptible to alteration by salty brines compared to crystalline, igneous components in the martian regolith. Because of the ultraxerous conditions (i.e., extremely dry and cold conditions, resulting in soils with very low moisture

[1]Carl Sagan Center, SETI Institute, Mountain View, CA 94043, USA. [2]Space Science and Astrobiology, NASA Ames Research Center, Moffett Field, CA 94035, USA. [3]Department of Chemistry, Umeå University, Umeå, Sweden. [4]Department of Geosciences, University of Montana, Missoula, MT 59812, USA. [5]Department of Geological Sciences, Stanford University, Stanford, CA 94305, USA. [6]Hawai'i Institute of Geophysics and Planetology, University of Hawai'i at Mānoa, Honolulu, HI 96822, USA. [7]Department of Earth & Space Sciences, University of Washington, Seattle, WA 98195, USA. [8]Lunar and Planetary Laboratory, University of Arizona, Tucson, AZ 85721, USA. [9]Astromaterials Research and Exploration Science, NASA Johnson Space Center, Houston, TX 77058, USA. [10]Department of Lithospheric Research, University of Vienna, Vienna, Austria.
*Corresponding author. Email: jbishop@seti.org

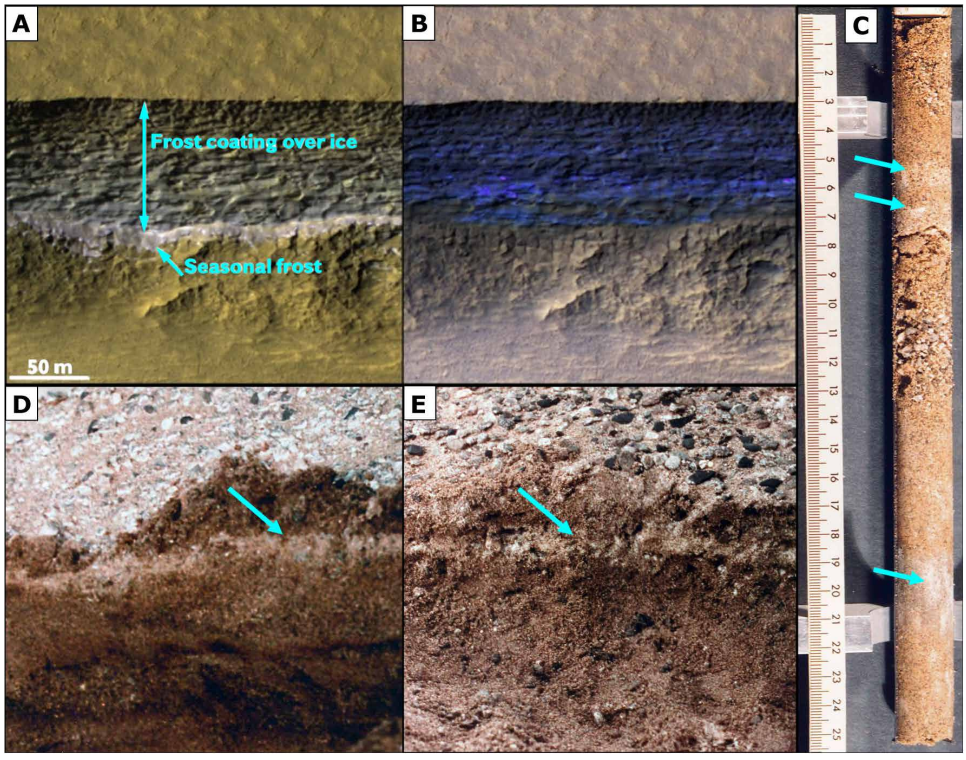

Fig. 1. Near-surface salts and ice. (**A**) Seasonal frost coating over ice at a scarp southeast of Hellas Planitia in early spring (*5*) from HiRISE image ESP_047338_1230 (56.6°S, 114.1°E). Image credit: NASA/JPL/University of Arizona. (**B**) View of (A) with an enhanced color stretch to emphasize the ice (blue shading). Image credit: NASA/JPL/University of Arizona. (**C**) Sediment core from the southern margin of Don Juan Pond, Wright Valley, Antarctica. Photo credit: Everett K. Gibson, NASA-JSC. (**D** and **E**) View of reddish, altered material below surface pebbles at soil pits on the southern margin of Don Juan Pond. Note the light-toned layers that are ~1 cm thick (cyan arrows) a few centimeters below the surface and occasionally also at deeper horizons. Photo credit: Everett K. Gibson, NASA-JSC.

content and high concentrations of soluble salts) on the surface of Mars, where surface temperatures rarely exceed 0°C, thin films of water, when available in near-surface environments, could be readily adsorbed by these short-range ordered phases.

RESULTS

Expansion and collapse caused by gypsum-chloride reactions

Chemical reactions of chlorides and Ca sulfates play an important role in geologic processes on Earth (Fig. 2 and fig. S7). Subsurface gypsum and halite deposits surrounding the Dead Sea in Israel are causing instability and sinkholes as they absorb groundwater (Fig. 2A). Halite hydration initiates deliquescence and then dissolves gypsum into the Cl brine, causing sediment gaps and subsequent collapse of overlying materials (*22*). Dissolution of subsurface gypsum beds in the halite-bearing Salar de Pajonales region of Chile produces hollow cavities 1 to 2 m deep (Fig. 2B). Many karst systems contain sulfates (including gypsum) that become destabilized in the presence of Cl salts. Disintegration of extensive gypsum deposits can form large caves, such as those at Carlsbad Caverns in New Mexico (*23*). Instability and collapse of caves and karst systems in Spain are attributed to dissolution of halite, gypsum, and glauberite [$Na_2Ca(SO_4)_2$] (*24*), while collapse features and debris flows on volcanic edifices are, in some cases, attributed to the presence of gypsum, for example, where large gypsum veins up to 10 m long are observed on the scarps exposed following edifice collapse (*25*). Thus, the interaction of water with gypsum and Cl salts appears to promote instability and mobility of surface materials in multiple natural environments.

In addition to geologic processes, reactions between chlorides and Ca sulfates produce expansion and collapse near salt mines, boreholes, and roadways. Gypsum is frequently used to stabilize roads but can expand and contract in the presence of Cl salts, causing roads to buckle (Fig. 2C and fig. S3, C and D) (*26*). Salt experiments revealed that reaction of gypsum with chlorides and phyllosilicates drives this process through the formation of oxychlorides that expand greatly (*26*).

To investigate hydration of subsurface salts on Mars, as well as the subsurface and surface distribution of hydrated salts and physical ramifications of subsurface water-salt interactions, we conducted laboratory experiments with altered volcanic material, Ca sulfate (Drierite), and Ca chloride (see Materials and Methods and figs. S2 and S3). These experiments began with the Ca sulfate in a dehydrated form similar to bassanite ($CaSO_4{\cdot}0.5H_2O$). The volcanic soil analog included abundant amorphous phases in a matrix of altered glass and basaltic grains (see Materials and Methods). In these experiments, soil-mineral mixtures were hydrated from below (Fig. 2D and figs. S4 and S5) to mimic activity of subsurface water on Mars. As liquid water was added to the system, it was adsorbed on the surfaces of the poorly crystalline aluminosilicates in the soil and absorbed by the sulfate grains. This was indicated by darkening of the soil from light brown to darker brown and by changing of the sulfate grain color from light blue to light pink (figs. S4 and S5). The Ca chloride grains likely also absorbed water, but this process could not be visually

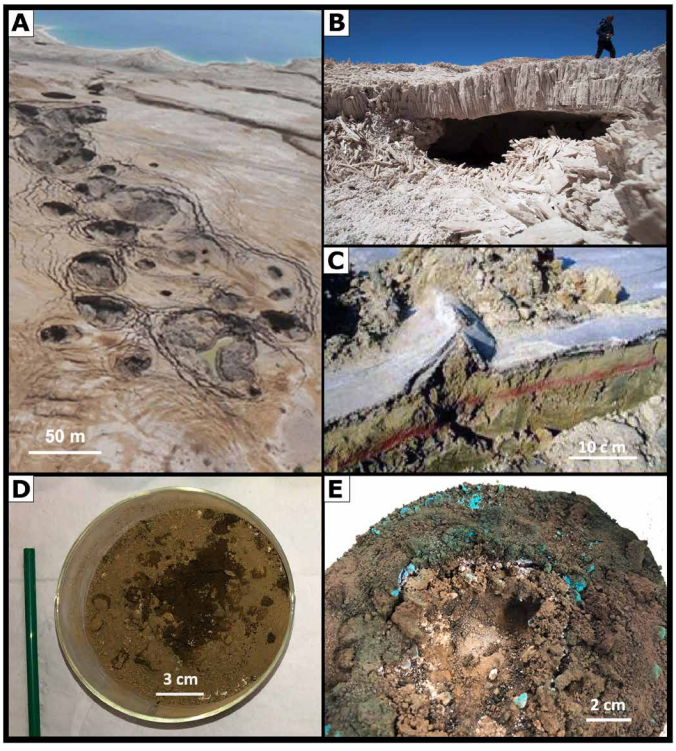

Fig. 2. Gypsum-salt expansion and collapse. (**A**) Sinkhole depressions produced by Cl salt reactions with gypsum in mud flat sediments at Wadi Ze'elim near the Dead Sea, Israel [modified from Yechieli *et al.* (*22*)]. Photo credit: Gideon Baer, Geological Survey of Israel. (**B**) Void space of 35 to 40 cm deep beneath gypsum beds at Salar de Pajonales, northern Chile. Note the deformation of the in-place gypsum beds (person for scale). Photo credit: Victor Robles Bravo, Campoalto. (**C**) Pavement distress caused by gypsum-salt expansion in lime- and cement-treated subsoils (*26*). Photo credit: Les Perrin, US Army Corps of Engineers. (**D** and **E**) Crust formation and soil expansion in Ca sulfate–$CaCl_2$ soil laboratory experiment. The Ca sulfate (Drierite) grains are blue when dry and pink when hydrated. Photo credit: Janice L. Bishop, SETI Institute.

confirmed in these experiments because Ca chloride remains white in more hydrated forms. During the experiment, salt solutions gradually migrated upward toward the surface, expanded, and collapsed to form raised crusts and cavities (Fig. 2E, fig. S5, and movie S1). Color indicators (see Materials and Methods) showed hydration of subsurface sulfates, while surface sulfates remained dry. This experiment provides an example of the expansion and collapse processes active in karst systems, evaporite environments, and roadways in multiple locations across Earth (e.g., Fig. 2, A to C, and fig. S3). This laboratory experiment and these natural settings demonstrate the disruptive ability of sulfates and Cl salts to expand and contract due to hydration, deliquescence, and dehydration. Although these examples do not replicate current martian conditions, similar processes could have occurred on Mars (e.g., in a setting such as Gale crater in an earlier environment when liquid water was present). In addition, even today on Mars, related processes could be occurring at a much slower pace in locations where thin films of liquid water or brine are present below the surface.

Martian salt observations

Elevated S and Cl levels have been identified in the soils on Mars and appear to be ubiquitous across much of the planet (*27*–*29*). S is assumed to be primarily present as sulfate on Mars with abundances typically ranging from 1 to 10 wt % SO_3 (*29*, *30*). Sulfate-enriched soils with up to 35 wt % SO_3 (including Ca sulfate, Mg sulfate, and Fe sulfate) were characterized by the Spirit rover at Paso Robles–type outcrops (*31*). Numerous hydrated sulfate outcrops have been detected on Mars from orbit using the Compact Reconnaissance Imaging Spectrometer for Mars (CRISM) instrument on the Mars Reconnaissance Orbiter spacecraft (*32*, *33*) including the Ca sulfates gypsum and bassanite, as well as a variety of monohydrated and polyhydrated sulfates. These can be distinguished by the shape and position of the hydration bands near 1.4 to 1.5, 1.9 to 2.0, and 2.4 μm (*34*–*36*). Several occurrences of Ca sulfates have been documented via spectral analyses from orbit: gypsum dunes at Olympia Undae (*37*), gypsum-bearing sediments at Noctis Labyrinthus (*38*), and bassanite at Mawrth Vallis (*39*).

Gypsum veins were observed at Endeavor crater using Pancam spectral hydration features near 934 to 1009 nm by Squyres *et al.* (*40*). Bassanite was detected in bright veins (*41*) in Gale crater sediments using the Chemistry and Camera (ChemCam) laser-induced breakdown spectroscopy (LIBS) instrument on the Mars Science Laboratory rover Curiosity. Sulfates are observed in all samples measured by CheMin at Gale crater (*21*, *30*), and gypsum, bassanite, and anhydrite are the most common crystalline sulfate salts observed there. Rapin *et al.* (*42*) report elevated Ca sulfate contents consistent with 30 to 50 wt % of these sulfates spanning 150 m of stratigraphy in the Murray formation using ChemCam LIBS data. Near the transition from the Sutton island member to the Blunts Point member, they observed a 10-m-thick horizon containing ~30 wt % Mg sulfates and lower Ca sulfate abundances.

Vaniman *et al.* (*30*) observed gypsum, bassanite, and anhydrite throughout Gale crater using CheMin XRD data. They noted that warm conditions (~6° to 30°C) inside the CheMin sample chamber acted to dehydrate gypsum present in the samples, producing bassanite over a period of sols during the XRD measurements. This was documented through decreasing gypsum abundance and increasing bassanite abundance over time for different samples, including a sample from Oudam, where no bassanite was initially present and where gypsum gradually decreased until, after 37 sols, it was absent and totally replaced by bassanite. All five samples containing gypsum experienced this dehydration to bassanite within a few sols. Vaniman *et al.* (*30*) propose that gypsum exposed on the surface at Gale crater during warmer seasons would have similarly experienced dehydration to bassanite over time. This is consistent with ChemCam analyses implying bassanite formation through diagenesis of gypsum veins (*41*). Gypsum is typically observed in samples where Ca sulfates are abundant including portions of the Murray formation, but only bassanite and anhydrite are observed in samples with lower sulfate abundance such as the Stimson sandstone (*30*). Revised estimates of the bulk Ca sulfate abundances determined using CheMin data by Rampe *et al.* (*43*) indicate the presence of these sulfates at several sampling locations with anhydrite generally in highest abundance (up to 21 wt %) and bassanite and gypsum varying from 1 to 7 wt %. These sulfate contents represent averages for a scoop of material delivered to CheMin and are lower than the 30 to 50 wt % Ca sulfates detected in point analyses by the ChemCam instrument (*42*).

Vaniman *et al.* (*30*) argue that some gypsum may have dehydrated to form anhydrite over time on Mars, but the pervasive anhydrite observed at Gale crater is more likely to have anhydrated directly

from solution. Although anhydrite generally forms at higher temperatures than gypsum in dilute fluids, concentrated brines enable formation of anhydrite at lower temperatures. Marion *et al.* (*44*) modeled anhydrite formation from concentrated sulfate brines at lower temperatures, even near freezing for high salt contents. Vaniman *et al.* (*30*) suggest that some hydration of anhydrate may have occurred to produce the mixed anhydrite-bassanite-gypsum occurrences, but because anhydrite is always present in these samples, Vaniman *et al.* (*30*) support low water/rock ratios and low temperatures hindering complete reaction to gypsum.

Cl was found to be widely distributed in the upper tens of centimeters of the martian regolith across equatorial and mid-latitude regions, at 0.49 wt % Cl, on average, by the Mars Odyssey GRS (*45*). Further, Keller *et al.* (*45*) found that Cl is not distributed homogeneously and varies by a factor of four with elevated concentrations, for example, at the Medusae Fossae formation. Chloride salts have been identified from orbit using spectral and thermophysical properties at over 600 distinct locations in low-albedo Noachian- and Hesperian-aged terrains (*33*, *46*, *47*) at 10 to 25 wt % abundance on the surface (*48*). Deposition in a lacustrine/playa setting or groundwater upwelling area are the favored formation theories (*47*, *48*). Chlorides detected at Terra Sirenum were deposited atop the ancient phyllosilicates and were likely mobilized and emplaced by near-surface waters (*49*). Perchlorate and chloride were both detected by the Phoenix Lander Wet Chemistry Laboratory, with perchlorate abundances at 0.6 to 0.7 wt % ClO_4^- and lower chloride abundances (*27*, *50*, *51*). Oxychloride salts (likely perchlorate and chlorate) are present at up to 1.2 wt % Cl abundance in the Cumberland mudstone at Gale crater (*52*) with lower abundances of perchlorate and oxychloride salts observed in other locations (*27*). The predominance of ClO_4^- over ClO_3^- in martian soils (*52*) is consistent with postdepositional processing and could imply limited availability of water since the emplacement of the oxychloride compounds (*53*). Cl levels detected in the soils at the Viking, Pathfinder, Opportunity, Spirit, and Curiosity landing sites generally vary from ~0.2 to 0.9 wt % Cl, with concentrations elevated by up to 3 to 4 wt % Cl in rare cases (*28*, *29*).

In situ analyses of regions thought to be rich in Cl and S salts on Mars could also provide clues to potential near-surface frozen or liquid brines because these salts can only be detected via orbital remote sensing if they occur at the surface. Stillman *et al.* (*10*) suggest that a layer of unconsolidated regolith is forming materials similar to caliche and is masking salt crusts, thus preventing their detection from orbit.

Solubility of Cl salts and brines

Characterization of the eutectic temperatures of Ca, Mg, and Na chlorides, chlorates, and perchlorates has shown that these Cl salts form brines well below 0°C (table S1). These eutectic temperatures indicate that brines could be occurring in subsurface environments on Mars where temperatures are −50° to −20°C or warmer. Thus, we investigated mixtures of Cl salts in an altered volcanic soil matrix to explain the capability of a salty Mars analog to form transient briny water in cold environments (Fig. 3). Low-temperature attenuated total reflectance (ATR) Fourier transform infrared (FTIR) spectroscopy experiments in the mid-IR region performed on our $CaCl_2$–basaltic soil matrix demonstrate changes in the H_2O stretching vibrations, a sensitive region for H—O—H bond length variations used to monitor H_2O ice, cryosalts, and their liquid phases in these samples. The basaltic Mars analog soil MK 91-16 used in these experiments contains primarily poorly crystalline and palagonitized basaltic glass (see Materials and Methods). At −90°C, where the sample is in a permafrost state (a), spectral bands are observed at 3380 and 3430 cm^{-1}, similar to those observed for flash-frozen $CaCl_2$ and H_2O ice solutions and mixtures, as well as bands and shoulder features near 3100 to 3250 cm^{-1}, where H_2O ice bands occur (Fig. 3A and fig. S1), as expected according to the $CaCl_2$ phase diagram shown in Fig. 3B. At −50° to −40°C, a partially liquid "slush" phase (b) formed following the eutectic temperature of $CaCl_2$ at about −51°C, where H—O—H vibrations due to H_2O ice and $CaCl_2/H_2O$ ice bands are progressively eliminated. The spectra in Fig. 3A show decreases in the bands at 3430 and 3380 cm^{-1} and a shift in the H_2O ice bands near 3225 and 3140 cm^{-1} toward higher wavenumbers. Further heating to −20°C (spectrum c) resulted in loss of these H_2O ice bands at 3225 and 3140 cm^{-1}. The spectral bands for the salty soil shift to a primary band at 3360 cm^{-1} with a weak shoulder near 3180 cm^{-1}, revealing deficiencies in the H-bonding network compared to the spectrum of either ice or liquid H_2O plus $CaCl_2$ and exhibiting strong similarities to the spectral properties of thin films of H_2O formed on micron-sized minerals at 25°C (*54*), and additional weak bands at 3490 and 3430 cm^{-1} (c). Molecular H_2O adsorbed on the surfaces of the poorly crystalline altered volcanic soil likely formed tiny pockets of H_2O ice in the flash-frozen sample that gradually began forming a liquid-like phase as the temperature rose to the eutectic point of $CaCl_2$ near −51°C. As the temperature continued to rise, these pockets of slush water/brine formed thin layers of water/brine along the surfaces of the poorly crystalline aluminosilicates in the altered volcanic soil matrix.

As the sample was heated to 20°C (d), spectral features shifted to 3490, 3450, and 3380 cm^{-1}, characteristic of water in a volcanic soil sample and $CaCl_2$ salts. In a separate experiment, we dried a portion of the $CaCl_2$–volcanic soil mixture at 25°C. After drying the sample for 172 min, the major spectral features observed were a doublet at 3490 and 3450 cm^{-1}, due to H—O—H stretching vibrations, and a doublet at 1628 and 1614 cm^{-1}, due to H—O—H bending vibrations that correspond to bound water in the sample. This is consistent with evaporation of excess adsorbed water by N_2(g) during the experiment, producing a desiccated $CaCl_2$–volcanic soil mixture (Fig. 3A) at 25°C. Related experiments demonstrate reaction of hydrated perchlorates with H_2O ice, whereby ice destabilization and weakening occur with as little as 10 volume % perchlorate (*55*). This diurnal cycling of Cl brines and reaction with H_2O ice could be contributing to interactions with sulfates and soil particles, as well as formation of crusts. Schematics of soil grains with ice and briny water for the (a) to (d) situations (Fig. 3C) depict the thin films of ice, liquid slush, or thin films of liquid water present in salty soils at these temperatures.

Phase diagrams (Fig. 3B) for $CaCl_2$ and Ca perchlorate mixtures (*56*) illustrate transitions from frozen H_2O ice and hydrated salts below about −51°C for $CaCl_2$ and below about −75°C for $Ca(ClO_4)_2$ to hydrated salts plus ice and/or solution, depending on the salt concentration. Ca oxychloride [e.g., chlorate (ClO_3^-) and perchlorate (ClO_4^-)] mixtures include liquids above the eutectic point for lower salt concentrations, while $CaCl_2$ mixtures include liquids above the eutectic for higher salt concentrations (fig. S6). Solubility calculations for low-temperature Ca-Cl-SO_4 systems (Fig. 4) indicate that antarcticite ($CaCl_2{\cdot}6H_2O$) is favored up to 0°C for high $CaCl_2$ concentrations, while ice (H_2O or frozen brine) and gypsum are favored at lower $CaCl_2$ concentrations.

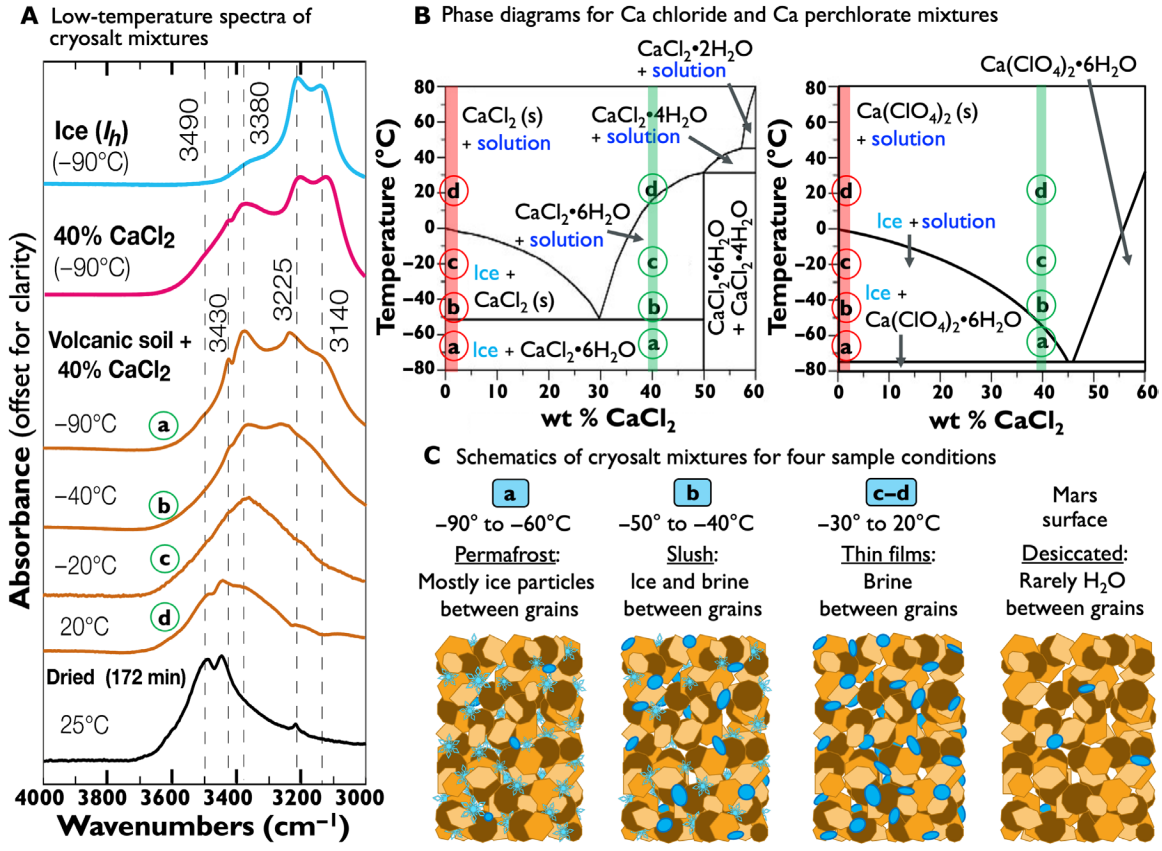

Fig. 3. Brine dissolution chemistry. (**A**) Low-temperature mid-IR ATR spectra of cryosalt mixtures where changes in the H_2O stretching vibration elucidate the nature of water in the system; (a) to (d) mark key shifts in this band associated with phase transformations in the frozen H_2O-$CaCl_2$ soil mixture. (**B**) Phase diagrams for $CaCl_2$ and $Ca(ClO_4)_2$ mixtures [after Marion *et al.* (*56*)] illustrating the path from (a) to (d); green marks 40 wt % $CaCl_2$ in the laboratory experiments, and red marks 1 to 4 wt % $CaCl_2$, which is more likely on Mars (*28*, *29*). (**C**) Schematics of cryosalt mixtures at four representative temperatures associated with different sample conditions: (a) "permafrost" where most of the water is frozen below about –60°C, (b) slush including a combination of frozen and liquid brine phases at about –50° to –40°C, (c) and (d) "thin films" of liquid H_2O/brine bound in interstitial sites between mineral grains observed near –30° to 20°C, and last, the case for a desiccated martian environment containing only limited water on grain surfaces.

Solubility calculations for gypsum in the presence of chlorides and perchlorates illustrate how interconnected these salts are (Fig. 5A). Gypsum solubility increases with increasing concentrations of Na and Mg chlorides and oxychlorides at typical Mars salt concentrations (*57*) but then salts out for high salt concentrations, resulting in lower gypsum solubility. In contrast, gypsum solubility decreases slightly with increasing Ca salt concentration, likely due to the common ion effect where competition for Ca is influencing gypsum and $CaCl_2$ or $Ca(ClO_4)_2$ solubility. Further, these solubility calculations demonstrate that $CaCl_2$ is more soluble than NaCl, $NaClO_4$, $MgCl_2$, or $Mg(ClO_4)_2$ in the presence of gypsum (Fig. 5A). While gypsum is mostly insoluble in the presence of $CaCl_2$, its solubility does vary with $CaCl_2$ abundance, and gypsum can release H_2O to form bassanite or anhydrite at low $CaCl_2$ concentrations (*57*). For a 1 to 4 wt % $CaCl_2$ solution (~0.09 to 0.36 M $CaCl_2$) on Mars, dissolution of ~0.01 mol/kg gypsum is predicted from Fig. 5. The presence of sulfates together with Cl salts would increase the number of hydrophilic sites, would enable more bonding of H_2O molecules on grain surfaces, and could help the entire system hold more water than with Cl salts alone. The temperature ranges of metastable partially liquid Cl salts are compared to the mean annual temperature of Mars in Fig. 5B. Only Mg and Ca perchlorates would be partially liquid all year round on

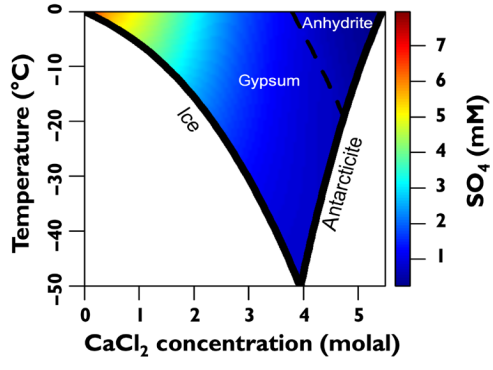

Fig. 4. Gypsum stability in $CaCl_2$ salt brines. Stability fields for gypsum, anhydrite, and antarcticite depending on both temperature and concentrations of $CaCl_2$ and SO_4, illustrating that phase diagrams for $CaCl_2$ systems become more complex in the presence of sulfates.

Mars (*58*), but all of these salts would be partially liquid for part of each day in summer. Previous modeling of sulfate-chloride systems suggests that resupply of water from deeper in the regolith could maintain a brine tens of centimeters below the surface for 10^7 years (*59*).

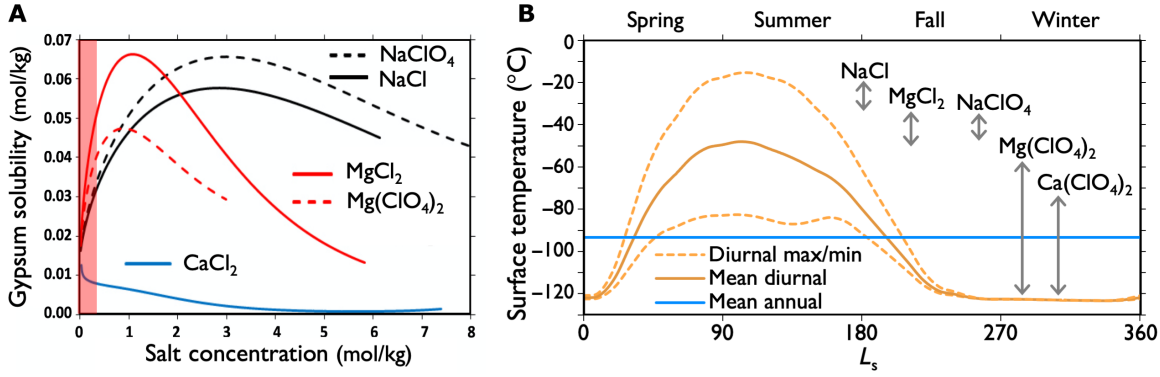

Fig. 5. Solubility diagrams for salts on Mars. (**A**) Gypsum solubility was calculated for variable concentrations of chlorides and perchlorates. The vertical red bar marks typical Cl concentrations in martian surface fines. Gypsum solubility for $Ca(ClO_4)_2$ is similar to that of $CaCl_2$. (**B**) Temperatures of metastable partially liquid Cl salts (gray arrows) compared to the mean annual temperature of Mars, the mean diurnal temperature, and the maximum and minimum diurnal temperatures, which are warmest in late spring and early summer [modified from Toner *et al.* (*58*)]. Only Mg and Ca perchlorates would be partially liquid all year round on Mars.

Repeated dehydration and hydration of Ca sulfates can result in microcrystalline gypsum coatings, bassanite or anhydrite inclusions within gypsum crystals, unusually shaped gypsum crystals, disruption of grains in confined spaces, breakage of the crystals, and development of fine-grained gypsum deposits (*60*). Laboratory experiments by Sievert *et al.* (*61*) showed that fine-grained anhydrite is less resistant to hydration than coarse grains. Their experiments demonstrate that after 50 hours of grinding in a ball mill apparatus, anhydrite grains were 85% altered to gypsum. Further, they observed that hydration of anhydrite is facilitated by the presence of Mg sulfate. Sievert *et al.* (*61*) propose a mechanism for conversion of anhydrite to gypsum during hydration through grinding. Processes proposed in this model could be occurring on Mars as well and are outlined in Fig. 6. According to this model, the outer parts of the anhydrite grains dissolve in the presence of water, creating a solution saturated with Ca^{2+} and SO_4^{2-} ions. These hydrated ions readsorb on the anhydrite grain surfaces, increasing the surface area of the grains and producing an outer layer of hydrated salts. Water molecules react preferentially with anhydrite rather than the adsorbed layer of hydrated $CaSO_4$ molecules, intensifying this cycle and increasing the thickness of the adsorbed hydrated salt layer. As the thickness of this adsorbed layer increases, cracks are formed from the surface toward the increasingly smaller anhydrite grain in the center. Sievert *et al.* (*61*) increased the rate of this cracking process through grinding. On Mars, this process could be facilitated by freeze-thaw cycling in a cold environment. Water molecules would then penetrate the cracks and more rapidly hydrate the remaining unaltered anhydrite. As the amount of hydrated $CaSO_4$ molecules increases, multiple tiny gypsum nuclei begin to form. These gypsum nucleation sites facilitate formation of gypsum, resulting in a nucleus with a gypsum crystal that rapidly grows from the layer of hydrated $CaSO_4$ molecules. Whether this process or another ultimately proceeds, it is difficult to retain fine-grained anhydrite in an "anhydrous" state under ambient conditions on Earth, and hydration of fine-grained anhydrite would also be likely in an aqueous environment on Mars.

Implications for martian surface and subsurface

Shallow water ice found across many mid-latitude (*5*, *6*) regions of Mars (Fig. 1, A and B) and water frost at several low-latitude pole-facing slopes in the southern hemisphere (*62*) could be supplying thin films of H_2O for salt reactions in the martian subsurface. Diurnal melting of thin layers of near-surface ice could provide liquid water (or slush) molecules that are gradually absorbed by Cl salts in the soil until a saturation point is reached and deliquescence occurs. Freeze-thaw cycles likely proceed on Mars as in MDV soils, where antarcticite forms below −51°C, coexists with H_2O ice at up to 50 wt % $CaCl_2$, and coexists with $CaCl_2{\cdot}4H_2O$ when $CaCl_2$ abundance exceeds 50 wt %. As the temperature rises, antarcticite would deliquesce on Mars as in the MDV. This Cl brine could then further dissolve Ca sulfates in the regolith, producing sinkholes as in the Dead Sea in Israel (Fig. 2A), void spaces as in Atacama salars (Fig. 2B), collapsing karst systems as in Spain (fig. S7A), and gaps in soil crusts as observed in laboratory experiments (Fig. 2E). This process would likely have required 100 to 300 ml of brine to dissolve 1 g of gypsum; thus, long-term, gradual melting of ice at a microscale on grain surfaces would be required to produce sufficient near-surface brine in the martian regolith for this process to change surface morphology. In addition, freeze-thaw cycles could facilitate reaction of the sulfates and Cl salts to form oxychlorides and complex hydrated Ca-Cl-SO_4 minerals that expand with great force and push up soil grains, creating surface crusts.

Seasonal flow features on Mars known as RSL have been observed across much of the planet (*8*), but RSL formation mechanisms remain enigmatic (*9*, *10*). These martian landslides are prevalent on sun-facing slopes (*8*) and are well documented across the equatorial regions and mid-latitudes of Mars (*8*) (Fig. 7); however, there is no consensus regarding wet or dry formation processes of these seasonally reappearing flows (*9*, *10*). Although mechanisms involving CO_2 frost (*9*) could be taking place at higher latitudes, equatorial RSL environments are too warm for this process. Furthermore, RSL form across bright bedrock, extend down over darker fan material at Coprates Chasma (Fig. 7B), and occur within and below gullies at Juventae Chasma (Fig. 7C and fig. S8) (*8*), where temperatures are consistently too warm for CO_2 frost to produce these features. RSL features also appear to be associated with Cl salts (*10*, *63*, *64*), although surface brines are not stable long term under current martian conditions and recharging Cl brines is problematic (*65*). Chlorides have been observed in numerous outcrops from orbit (*46*) at 10 to 25 wt % (*48*), and Cl salts have been identified in martian soils by every rover at ~0.5 to 1.5 wt % Cl (*27*), equivalent to ~1 to 4 wt % halite or $CaCl_2$. Recent characterization of equatorial mass wasting indicates that it is most common in sulfate-rich sediments (*66*), suggesting that these

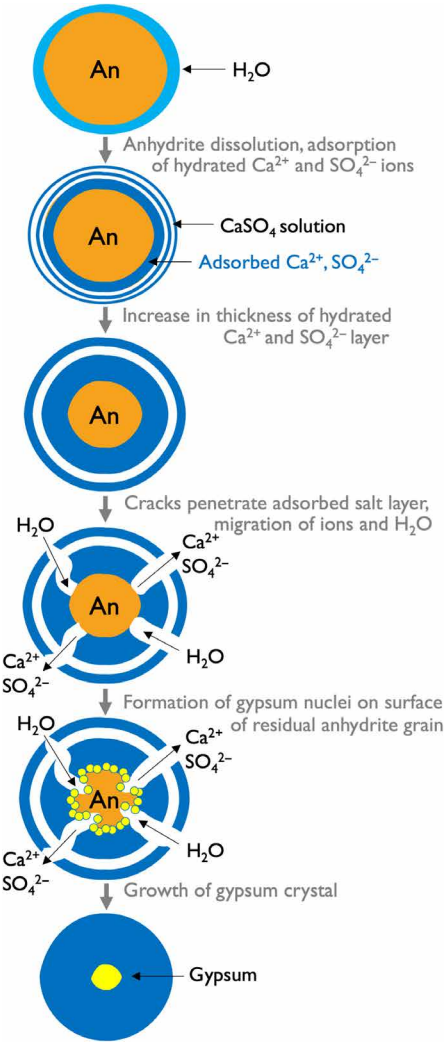

Fig. 6. Diagram of anhydrite hydration. Grains of anhydrite exposed to thin layers of liquid H_2O on their surfaces would gradually dissolve, and liberated Ca^{2+} and SO_4^{2-} ions would hydrate and adsorb on the grain surfaces. Gradually, this adsorbed hydrated salt layer thickens, and then cracks penetrate through this salt layer, enabling flow of water and ions deeper into the remaining anhydrite grain. Last, gypsum nuclei crystallize along the residual anhydrite grain, and a gypsum crystal forms [after diagram by Sievert *et al.* (*61*)].

outcrops are less stable. In addition, a high density of relatively long RSL is observed in bright layered deposits in Valles Marineris where sulfate abundance is high (*10*). Multiple hydrated sulfates have been detected from orbit (*33*) including Ca sulfates at Mawrth Vallis (*39*) and the Valles Marineris region (*38*), and instruments on the Curiosity rover have detected anhydrite, bassanite, and gypsum at Gale crater (*21*, *30*, *41*).

Another complexity to martian RSL formation is their increased activity following dust storms (*67*). For this study, we considered the association of RSL with sulfates, Cl salts, and dust storms and developed a model whereby dust loading on fragile surface crusts (that formed via the action of thin water films on salty soils) leads to slumping of surface material and landslides on sloped surfaces. Figure 8 illustrates how these salts could react in the martian subsurface and how progressive expansion and collapse could produce a fragile network of crusted material at the surface. Repeated freeze-thaw cycling and expansion/contraction of salty near-surface soils on Mars would produce small-scale depressions and raised surface crusts. These projections of crusted soil particles would be vulnerable to physical alteration from impact gardening, wind abrasion, and dust storms on Mars and become unstable, loosely bound networks of formerly crusted material at sites where salts are present just below the surface. Because the number of RSL features increases following dust storms (*67*), there appears to be a link between dust deposition and RSL activity. Dust loading on these fragile crusts during dust storms could induce collapse of the surface features and tumbling of particles downslope. According to our model, as this process proceeds, loose, fractured surface material slides downward producing landslides and leaving RSL tracks marking locations of former salt crusts. Some gullies may also be related to near-surface brines and salt crusts, and the larger scale of debris flows observed for gullies could be initiated through this process as well. Our model benefits from subsurface recycling of the Cl-rich salt to brine to salt system, where liquid water is not released on the surface. Most of the activity of the Cl salts and sulfates occurs below the surface and would not be detectable from orbit; however, regions that do contain elevated sulfate abundances on the surface (including Valles Marineris) would be expected to contain sulfates below the surface as well. Subsurface Cl salts in these sulfate-rich regions could trigger brine flow and drive the processes leading to landslides and RSL.

Tracking of RSL features using morning images from the Colour and Stereo Surface Imaging System on European Space Agency (ESA's) ExoMars Trace Gas Orbiter and afternoon images from HiRISE revealed RSL activity on steep slopes in Hale crater where local temperatures are sufficiently warm for melting of water ice and deliquescence of Cl salts (*68*). Thermal modeling and remote sensing observations support a hybrid model for RSL formation at Hale crater whereby subsurface deliquescence of salts produces liquid H_2O, but dry flows on the surface are responsible for the RSL (*68*, *69*).

DISCUSSION

This study illustrates the disruptive potential of sulfate-chloride reactions in laboratory experiments and in the field and depicts how these salt brines could be contributing to RSL formation. Low-temperature spectroscopy experiments demonstrate formation of thin films of liquid water or slush water in a cold, partly liquid system at −40° to −20°C on mineral grains mixed with $CaCl_2$ in the laboratory, consistent with observations of subsurface liquid water in gypsum- and halite-bearing Antarctic sediments. Similarly, near-surface salts would enable subsurface mobility of thin films of liquid water around grain surfaces on Mars. Experiments and modeling of Cl salts and sulfates indicate that integrating these salt components provides more complex hydration behavior and facilitates formation of low-temperature brines. Although we tested $CaCl_2$ and Ca sulfates in our experiment with volcanic ash, reaction of Mg sulfates with altered volcanic material by Vaniman and Chipera (*70*) demonstrated extraction of Ca from palagonitized material and formation of gypsum. This suggests that fine-grained gypsum and other Ca sulfates may be formed on Mars in poorly crystalline or palagonitized materials in the regolith where other sulfates are present. Sievert *et al.* (*61*) also noted increasing gypsum formation from anhydrite in the presence of Mg sulfate. Our laboratory wet/dry cycling experiments with Ca sulfate and $CaCl_2$ salt horizons in volcanic soil reveal mobility of salts through the strata, crust formation, surface uplift,

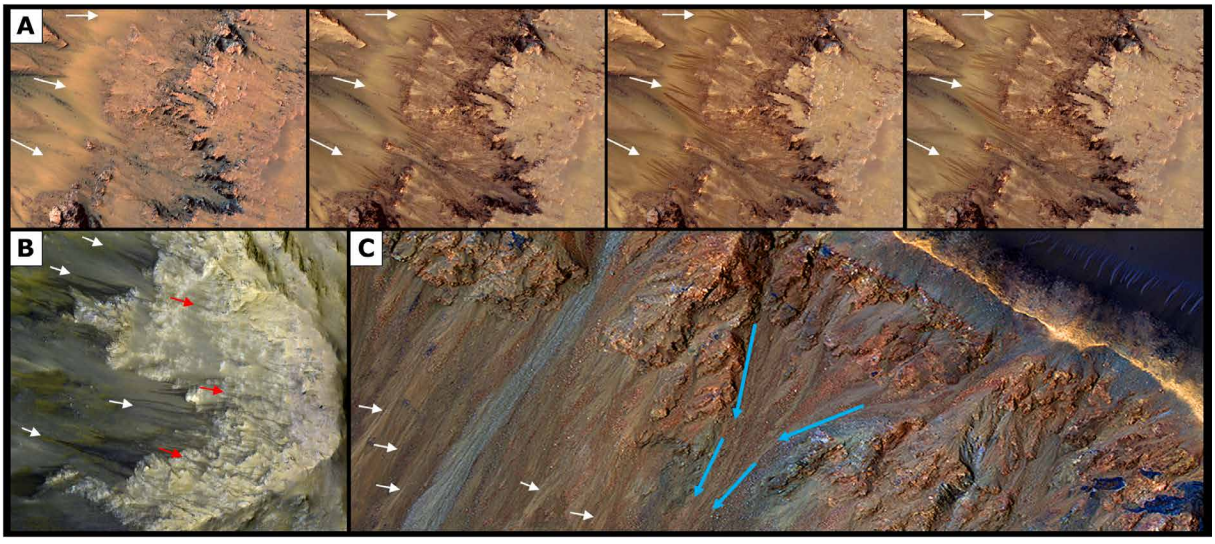

Fig. 7. Mobilization of surface material by RSL. (**A**) Enhanced color views demonstrating RSL development (white arrows) over time at Palikir crater (inside Newton Basin) (*79*) for Mars years 29 to 30; HiRISE images ESP_011428_1380, ESP_022267_1380, ESP_022689_1380, and ESP_022834_1380. (**B**) RSL flowing first over bright bedrock (red arrows) and then over the darker fan (white arrows) in Coprates Chasma (*8*); HiRISE image ESP_050021_1670. (**C**) RSL (white arrows) within and below gullies (blue arrows) on a hillside within Juventae Chasma (*8*); enhanced color view from HiRISE ESP_ 032496_1755. Image credit: NASA/JPL/University of Arizona.

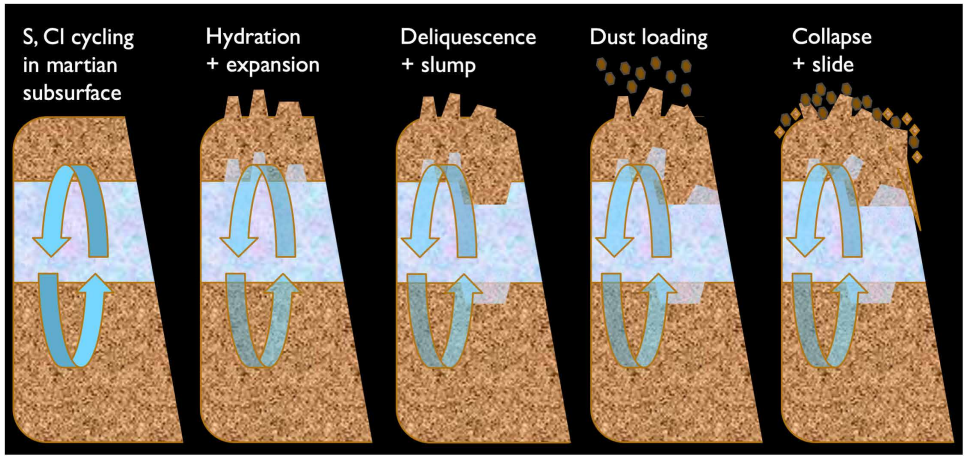

Fig. 8. Model of near-surface martian cryosalt modification. Potential brine-crust processes taking place in the near-surface region on Mars as ice melts and brine circulates, causing hydration, expansion, deliquescence, slumping and dust loading on fragile surfaces, collapse, and landslides.

and collapse features, mimicking formation of sinkholes, cave collapse, debris flows, and surface upheave in several environments on Earth. These observations support our hypothesis of microscale liquid brines arising from freeze/thaw cycling, salt deliquescence, and slush water formation, with no visible liquid water or brine on the surface. These brine expansion and contraction events occurred in environments much more hydrated than Mars, although these events have been observed in multiple moisture environments including the arid regions of the Atacama Desert. On geologic time scales, these microscale expansion and contraction events would likely occur on Mars at a slow but continual pace to accumulate disrupted surfaces. Our model proposes that slow brine events over long time periods interact with altered, fine-grained basaltic grains to produce fragile surfaces that become dehydrated and sand blasted in the harsh martian surface environment. We hypothesize that these fragile surfaces collapse following dust loading, producing landslide features visible from orbit. This model provides a link between dust storms and the increase in RSL observations following these storms but needs to be tested further.

This model describes a hybrid mechanism for RSL formation, whereby both wet and dry actions contribute to these landslide features. Our model requires near-surface liquid brines at the molecular level to provide salt mobility that disrupts the surface materials, preparing a vulnerable surface. These fragile surfaces could be prepared over thousands or millions of years in regions where near-surface ice and salts are present. Repeated dust loading at the same or nearby sites in subsequent seasons could produce additional instability and new or lengthening flow features. Our model suggests a source of near-surface water ice, Cl salts, and sulfates below the top of the RSL features. This is consistent with observations of sulfates from orbit in some

regions where RSL are observed, but unfortunately, subsurface minerals cannot be detected via orbital remote sensing. This model can be tested once we send a surface mission to a site exhibiting RSL activity.

MATERIALS AND METHODS

Experimental design

This study includes low-temperature spectra of cryosalt mixtures as Mars analogs to investigate changes in the spectral properties of salty permafrost as it liquefies. Solubility calculations were performed to determine relationships among Cl salts and sulfates in the Mars analog samples considered. Soil-salt crust experiments were performed to monitor changes in a Mars analog regolith through wet/dry cycling and adsorption of water by the Ca chloride and Ca sulfate in the analog regolith.

Low-temperature ATR-FTIR experiments

Mixtures of Cl salts and Mars analog soils were prepared for earlier studies to characterize the visible/near-IR spectral properties of $CaCl_2$ and Mg and Fe perchlorates in a volcanic soil matrix (*71*). The low-temperature ATR spectra covering the H—O—H stretching spectral region shown in Fig. 3A and fig. S1 were measured with a Bruker Vertex 70/V FTIR spectrometer equipped with a Deuterated L-Alanine Doped Triglycine Sulfate (DLaTGS) detector. Measurements were performed over the spectral range of 600 to 4000 cm^{-1} with a spectral resolution of 4 cm^{-1} using a 10-Hz forward/reverse scanning rate. The Blackman-Harris three-term apodization function at 16 cm^{-1} phase resolution was used with the Mertz phase correction algorithm. These spectral parameters were developed for previous experiments exploring thin films of water on fine-grained mineral surfaces (*72*) to obtain a better signal/noise ratio. A 10-μl droplet of aqueous solutions (H_2O and $CaCl_2$) and aliquots of wet pastes of volcanic soil–salt mixtures were applied directly onto the precooled ATR thermal stage (Golden Gate, serial number N29328 by Specac) at −90°C. The temperature was retained at −90°C for 15 min to confirm the formation of a stable frozen volcanic soil–brine mixture. The volcanic soil sample used here is MK 91-16 described in more detail for the crust experiments below. These spectra collected of flash-frozen droplets of H_2O ice, $CaCl_2$, and volcanic soil mixtures containing 40% $CaCl_2$ were taken at −90°C by averaging 100 scans for each spectrum over a period of 89 s. The temperature was then raised gradually to 25°C using a heating rate of 10°C/min while recording a spectrum every 3 s to monitor instantaneous changes as a function of temperature.

For the last part of this experiment, we dried the volcanic soil plus 40% $CaCl_2$ mixture under purified air at 25°C for 172 min using the same instrument with identical spectral resolution and parameters for the first part of the experiment. We coadded 100 scans, producing an average spectrum every 89 s.

All spectral data were offset at 4000 cm^{-1} and treated using a model-free chemometric analysis technique called multivariate curve resolution alternating least square (MCR-ALS) analysis (*73*). MCR-ALS enables treatment of the spectral data with the single value decomposition method to reduce noise in the collected spectra (*54*). All of the spectral data analysis and chemometrics were performed using the MATLAB (9.6.0) environment.

Solubility and salt mobility determinations

The solubility determinations for gypsum and Cl salts were calculated using the model developed by Toner *et al.* (*57*). Studies of salts in MDV sediments have estimated that brines migrate in frozen soils there at rates of ~10^{-9} cm/s (*74*). Assuming a slower rate for Mars due to colder conditions, ~10^{-11} cm/s was estimated. Using a nominal salt concentration of 0.01 g/cm^3 soil based on the Phoenix Lander Wet Chemistry Laboratory experiments (*75*, *76*), a salt flux of ~10^{-13} g of salt/s per cubic centimeter soil was used. This estimate of salt concentration is likely lower than Cl salts present in equatorial locations on Mars based on Cl detections by GRS in the upper tens of centimeters of the regolith (*45*), and it is substantially lower than the 10 to 25 wt % chloride predicted (*48*) in regions where chlorides are observed from orbit (*33*). This translates to a deflation rate of 5×10^{-12}% per s, 0.00002-mm deflation per year, or 2-cm deflation in 1 million years, which was assumed to be a lower limit.

Crust experiments

The soil-salt crust experiments were performed at the SETI Institute to test hydration, reaction, and mobility of sulfates and Cl salts (*77*). For these experiments, an altered volcanic ash from Mauna Kea (MK 91-16) composed of ~85 wt % X-ray amorphous material including poorly crystalline aluminosilicates, altered glass, and altered mafic grains with basaltic composition (*78*) was used as an analog Mars regolith. The ash sample was dry sieved to <2 mm to remove larger fragments but was dominated by fine-grained material as illustrated by scanning electron microscopy images of this sample (fig. S2). Drierite [Ca sulfate spiked with Co(II) chloride as a color indicator] was used as the sulfate in these experiments due to its changing color with hydration state (fig. S3). A 1-cm-thick layer of the <2-mm fraction of Mauna Kea soil was placed in a glass dish and covered with ground (<500 μm) dried Drierite, dried Drierite pellets (~3 to 5 mm in diameter), and ground (<500 μm) $CaCl_2{\cdot}2H_2O$, and then another 1.5-cm-thick layer of Mauna Kea soil was placed on top (figs. S4 and S5). Water was added to the system via a straw inserted through the material to the bottom of the glass dish. The dry soil and salts absorbed the H_2O within a few seconds (Fig. 2D and movie S1). With the addition of water (10 ml at a time at 10- to 15-min intervals for a total of 70 ml), a hole in the center of the soil/salt system formed, and water spread across the bottom of the glass dish. Gradually, the salt layer at the bottom turned pink as it hydrated, cracks formed in the soil (perhaps due to dissolution of the salts), and the salts migrated both up and down through the layers as water was absorbed by the salts (see figs. S3 to S5). Fine-grained anhydrite could have been used instead of the bassanite-like dried Drierite, but anhydrite may have taken longer to hydrate than bassanite, and using Drierite was convenient for monitoring hydration changes through changes in color.

This experiment was conducted under ambient laboratory conditions to complete the reactions in a feasible time frame. Our low-temperature IR experiments on $CaCl_2$ mixed with this martian soil analog, largely composed of poorly crystalline materials, illustrated that liquid water/brine is present in this system under cold temperatures, down to about −30°C, providing confidence that similar reactions could have occurred under colder temperatures such as those present on Mars, albeit at a slower pace. Following absorption of the water by the soil-salt mixture, the crust material was air-dried in the laboratory for 1 hour and then heated to facilitate dehydration of the crust sample. After heating the crust at intervals of 15 min at 100°C for 1 hour and then air-drying the crust in the laboratory for a day, the surface material became dry (blue Drierite representing bassanite) and very hard, while subsurface material stayed slightly

hydrated (pink Drierite representing gypsum) (Fig. 2E, fig. S5, and movie S1) (*77*). We acknowledge that future experiments performed under Mars-like conditions over longer time periods could provide additional scope to these kinds of reactions taking place in near-surface martian environments (*59*).

SUPPLEMENTARY MATERIALS

Supplementary material for this article is available at http://advances.sciencemag.org/cgi/content/full/7/6/eabe4459/DC1

REFERENCES AND NOTES

1. J. L. Bishop, A. G. Fairén, J. R. Michalski, L. Gago-Duport, L. L. Baker, M. A. Velbel, C. Gross, E. B. Rampe, Surface clay formation during short-term warmer and wetter conditions on a largely cold ancient Mars. *Nat. Astron.* **2**, 206–213 (2018).
2. R. M. Haberle, C. P. McKay, J. Schaeffer, N. A. Cabrol, E. A. Grin, A. P. Zent, R. Quinn, On the possibility of liquid water on present-day Mars. *J. Geophys. Res. Planets* **106**, 23317–23326 (2001).
3. R. D. Wordsworth, The climate of early Mars. *Annu. Rev. Earth Planet. Sci.* **44**, 381–408 (2016).
4. P. H. Smith, L. K. Tamppari, R. E. Arvidson, D. Bass, D. Blaney, W. V. Boynton, A. Carswell, D. C. Catling, B. C. Clark, T. Duck, E. DeJong, D. Fisher, W. Goetz, H. P. Gunnlaugsson, M. H. Hecht, V. Hipkin, J. Hoffman, S. F. Hviid, H. U. Keller, S. P. Kounaves, C. F. Lange, M. T. Lemmon, M. B. Madsen, W. J. Markiewicz, J. Marshall, C. P. McKay, M. T. Mellon, D. W. Ming, R. V. Morris, W. T. Pike, N. Renno, U. Staufer, C. Stoker, P. Taylor, J. A. Whiteway, A. P. Zent, H_2O at the Phoenix landing site. *Science* **325**, 58–61 (2009).
5. C. M. Dundas, A. M. Bramson, L. Ojha, J. J. Wray, M. T. Mellon, S. Byrne, A. S. McEwen, N. E. Putzig, D. Viola, S. Sutton, E. Clark, J. W. Holt, Exposed subsurface ice sheets in the martian mid-latitudes. *Science* **359**, 199–201 (2018).
6. S. Piqueux, J. Buz, C. S. Edwards, J. L. Bandfield, A. Kleinböhl, D. M. Kass, P. O. Hayne, Widespread shallow water ice on Mars at high latitudes and midlatitudes. *Geophys. Res. Lett.* **46**, 14290–14298 (2019).
7. D. R. Lowe, J. L. Bishop, D. Loizeau, J. J. Wray, R. A. Beyer, Deposition of >3.7 Ga clay-rich strata of the Mawrth Vallis Group, Mars, in lacustrine, alluvial, and aeolian environments. *GSA Bull.* **132**, 17–30 (2020).
8. A. S. McEwen, in *From Habitability to Life on Mars*, N. A. Cabrol, E. A. Grin, Eds. (Elsevier, 2017), pp. 249–274.
9. C. M. Dundas, A. S. McEwen, M. Chojnacki, M. P. Milazzo, S. Byrne, J. N. McElwaine, A. Urso, Granular flows at recurring slope lineae on Mars indicate a limited role for liquid water. *Nat. Geosci.* **10**, 903–907 (2017).
10. D. E. Stillman, T. I. Michaels, R. E. Grimm, Characteristics of the numerous and widespread recurring slope lineae (RSL) in Valles Marineris, Mars. *Icarus* **285**, 195–210 (2017).
11. E. C. Morris, H. E. Holt, T. A. Mutch, J. F. Lindsay, Mars analog studies in Wright and Victoria Valleys, Antarctica. *Antarct. J.* **7**, 113–114 (1972).
12. W. W. Dickinson, R. H. Grapes, Authigenic chabazite and implications for weathering in Sirius Group diamictite, Table Mountain, Dry Valleys, Antarctica. *J. Sediment. Res.* **67**, 815–820 (1997).
13. F. C. Ugolini, D. M. Anderson, Ionic migration and weathering in frozen Antarctic soils. *Soil Sci.* **115**, 461–470 (1973).
14. G. G. C. Claridge, I. B. Cambpell, The salts in Antarctic soils, their distribution and relationship to soil processes. *Soil Sci.* **123**, 377–384 (1977).
15. E. K. Gibson, S. J. Wentworth, D. S. McKay, Chemical weathering and diagenesis of a cold desert soil from Wright Valley, Antarctica: An analog of martian weathering processes. *J. Geophys. Res.* **88**, A912–A928 (1983).
16. P. Englert, J. L. Bishop, E. K. Gibson, C. Koeberl, Subsurface salts in Antarctic Dry Valley soils, in *44th Lunar Planetary Science Conference*, The Woodlands, TX (Lunar and Planetary Institute, 2013), Abstract #1804.
17. Z. F. M. Burton, J. L. Bishop, P. Englert, C. Koeberl, E. K. Gibson, Salts and clays beneath surface sediments in Antarctica provide clues to weathering and geochemistry of Mars, in *50th Lunar Planetary Science Conference*, The Woodlands, TX (Lunar and Planetary Institute, 2019), Abstract #1766.
18. J. L. Bishop, P. A. J. Englert, S. Patel, D. Tirsch, A. J. Roy, C. Koeberl, U. Böttger, F. Hanke, R. Jaumann, Mineralogical analyses of surface sediments in the Antarctic Dry Valleys: Coordinated analyses of Raman spectra, reflectance spectra and elemental abundances. *Philos. Trans. R. Soc. A* **372**, 20140198 (2014).
19. R. P. Sharp, M. C. Malin, Surface geology from Viking landers on Mars: A second look. *GSA Bull.* **95**, 1398–1412 (1984).
20. P. R. Christensen, Regional dust deposits on Mars: Physical properties, age, and history. *J. Geophys. Res.* **91**, 3533–3545 (1986).
21. T. F. Bristow, E. B. Rampe, C. N. Achilles, D. F. Blake, S. J. Chipera, P. Craig, J. A. Crisp, D. J. Des Marais, R. T. Downs, R. Gellert, J. P. Grotzinger, S. Gupta, R. M. Hazen, B. Horgan, J. V. Hogancamp, N. Mangold, P. R. Mahaffy, A. C. McAdam, D. W. Ming, J. M. Morookian, R. V. Morris, S. M. Morrison, A. H. Treiman, D. T. Vaniman, A. R. Vasavada, A. S. Yen, Clay mineral diversity and abundance in sedimentary rocks of Gale crater, Mars. *Sci. Adv.* **4**, eaar3330 (2018).
22. Y. Yechieli, M. Abelson, G. Baer, Sinkhole formation and subsidence along the Dead Sea coast, Israel. *Hydrogeol. J.* **24**, 601–612 (2016).
23. J. B. Epstein, *National Evaporite Karst—Some Western Examples* (U.S. Geological Survey, 2005).
24. F. Gutiérrez, I. Fabregat, C. Roqué, D. Carbonel, J. Guerrero, F. García-Hermoso, M. Zarroca, R. Linares, Sinkholes and caves related to evaporite dissolution in a stratigraphically and structurally complex setting, Fluvia Valley, eastern Spanish Pyrenees. Geological, geomorphological and environmental implications. *Geomorphology* **267**, 76–97 (2016).
25. D. R. Zimbelman, R. O. Rye, G. N. Breit, Origin of secondary sulfate minerals on active andesitic stratovolcanoes. *Chem. Geol.* **215**, 37–60 (2005).
26. A. J. Puppala, S. S. C. Congress, N. Talluri, E. Wattanasanthicharoen, Sulfate-heaving studies on chemically treated sulfate-rich geomaterials. *J. Mater. Civil Eng.* **31**, 04019076 (2019).
27. B. Sutter, R. C. Quinn, P. D. Archer, D. P. Glavin, T. D. Glotch, S. P. Kounaves, M. M. Osterloo, E. B. Rampe, D. W. Ming, Measurements of oxychlorine species on Mars. *Int. J. Astrobiol.* **16**, 203–217 (2017).
28. B. C. Clark, A. K. Baird, R. J. Weldon, D. M. Tsusaki, L. Schnabel, M. P. Candelaria, Chemical composition of martian fines. *J. Geophys. Res.* **87**, 10059–10067 (1982).
29. R. Gellert, A. S. Yen, in *Remote Compositional Analysis: Techniques for Understanding Spectroscopy, Mineralogy, and Geochemistry of Planetary Surfaces,* J. L. Bishop, J. F. Bell III, J. E. Moersch, Eds. (Cambridge Univ. Press, 2020), pp. 555–572.
30. D. T. Vaniman, G. M. Martínez, E. B. Rampe, T. F. Bristow, D. F. Blake, A. S. Yen, D. W. Ming, W. Rapin, P.-Y. Meslin, J. M. Morookian, R. T. Downs, S. J. Chipera, R. V. Morris, S. M. Morrison, A. H. Treiman, C. N. Achilles, K. Robertson, J. P. Grotzinger, R. M. Hazen, R. C. Wiens, D. Y. Sumner, Gypsum, bassanite, and anhydrite at Gale crater, Mars. *Am. Mineral.* **103**, 1011–1020 (2018).
31. A. S. Yen, R. V. Morris, B. C. Clark, R. Gellert, A. T. Knudson, S. Squyres, D. W. Mittlefehldt, D. W. Ming, R. Arvidson, T. McCoy, M. Schmidt, J. Hurowitz, R. Li, J. R. Johnson, Hydrothermal processes at Gusev Crater: An evaluation of Paso Robles class soils. *J. Geophys. Res. Planets* **113**, E06S10 (2008).
32. S. L. Murchie, J. F. Mustard, B. L. Ehlmann, R. E. Milliken, J. L. Bishop, N. K. McKeown, E. Z. Noe Dobrea, F. P. Seelos, D. L. Buczkowski, S. M. Wiseman, R. E. Arvidson, J. J. Wray, G. Swayze, R. N. Clark, D. J. Des Marais, A. S. McEwen, J.-P. Bibring, A synthesis of martian aqueous mineralogy after 1 Mars year of observations from the Mars Reconnaissance Orbiter. *J. Geophys. Res. Planets* **114**, E00D06 (2009).
33. B. L. Ehlmann, C. S. Edwards, Mineralogy of the martian surface. *Annu. Rev. Earth Planet. Sci.* **42**, 291–315 (2014).
34. J. L. Bishop, M. Parente, C. M. Weitz, E. Z. Noe Dobrea, L. H. Roach, S. L. Murchie, P. C. McGuire, N. K. McKeown, C. M. Rossi, A. J. Brown, W. M. Calvin, R. Milliken, J. F. Mustard, Mineralogy of Juventae Chasma: Sulfates in the light-toned mounds, mafic minerals in the bedrock, and hydrated silica and hydroxylated ferric sulfate on the plateau. *J. Geophys. Res. Planets* **114**, E00D09 (2009).
35. J. L. Bishop, M. D. Lane, M. D. Dyar, S. J. King, A. J. Brown, G. Swayze, Spectral properties of Ca-sulfates: Gypsum, bassanite and anhydrite. *Am. Mineral.* **99**, 2105–2115 (2014).
36. M. D. Lane, J. L. Bishop, M. D. Dyar, T. Hiroi, S. A. Mertzman, D. L. Bish, P. L. King, A. D. Rogers, Mid-infrared emission spectroscopy and visible/near-infrared reflectance spectroscopy of Fe-sulfate minerals. *Am. Mineral.* **100**, 66–82 (2015).
37. Y. Langevin, F. Poulet, J.-P. Bibring, B. Gondet, Sulfates in the north polar region of Mars detected by OMEGA/Mars Express. *Science* **307**, 1584–1586 (2005).
38. C. M. Weitz, J. L. Bishop, J. A. Grant, Gypsum, opal, and fluvial channels within a trough of Noctis Labyrinthus, Mars: Implications for aqueous activity during the Late Hesperian to Early Amazonian. *Planet. Space Sci.* **87**, 130–145 (2013).
39. J. J. Wray, S. W. Squyres, L. H. Roach, J. L. Bishop, J. F. Mustard, E. Z. Noe Dobrea, Identification of the Ca-sulfate bassanite in Mawrth Vallis, Mars. *Icarus* **209**, 416–421 (2010).
40. S. W. Squyres, R. E. Arvidson, J. F. Bell III, F. Calef III, B. C. Clark, B. A. Cohen, L. A. Crumpler, P. A. de Souza Jr., W. H. Farrand, R. Gellert, J. Grant, K. E. Herkenhoff, J. A. Hurowitz, J. R. Johnson, B. L. Jolliff, A. H. Knoll, R. Li, S. McLennan, D. W. Ming, D. W. Mittlefehldt, T. J. Parker, G. Paulsen, M. S. Rice, S. W. Ruff, C. Schröder, A. S. Yen, K. Zacny, Ancient impact and aqueous processes at Endeavour Crater, Mars. *Science* **336**, 570–576 (2012).
41. W. Rapin, P.-Y. Meslin, S. Maurice, D. Vaniman, M. Nachon, N. Mangold, S. Schröder, O. Gasnault, O. Forni, R. C. Wiens, G. M. Martínez, A. Cousin, V. Sautter, J. Lasue, E. B. Rampe, D. Archer, Hydration state of calcium sulfates in Gale crater, Mars: Identification of bassanite veins. *Earth Planet. Sci. Lett.* **452**, 197–205 (2016).
42. W. Rapin, B. L. Ehlmann, G. Dromart, J. Schieber, N. H. Thomas, W. W. Fischer, V. K. Fox, N. T. Stein, M. Nachon, B. C. Clark, L. C. Kah, L. Thompson, H. A. Meyer, T. S. J. Gabriel, C. Hardgrove, N. Mangold, F. Rivera-Hernandez, R. C. Wiens, A. R. Vasavada, An interval of high salinity in ancient Gale crater lake on Mars. *Nat. Geosci.* **12**, 889–895 (2019).

43. E. B. Rampe, D. F. Blake, T. F. Bristow, D. W. Ming, D. T. Vaniman, R. V. Morris, C. N. Achilles, S. J. Chipera, S. M. Morrison, V. M. Tu, A. S. Yen, N. Castle, G. W. Downs, R. T. Downs, J. P. Grotzinger, R. M. Hazen, A. H. Treiman, T. S. Peretyazhko, D. J. Des Marais, R. C. Walroth, P. I. Craig, J. A. Crisp, B. Lafuente, J. M. Morookian, P. C. Sarrazin, M. T. Thorpe, J. C. Bridges, L. A. Edgar, C. M. Fedo, C. Freissinet, R. Gellert, P. R. Mahaffy, H. E. Newsom, J. R. Johnson, L. C. Kah, K. L. Siebach, J. Schieber, V. Z. Sun, A. R. Vasavada, D. Wellington, R. C. Wiens, Mineralogy and geochemistry of sedimentary rocks and eolian sediments in Gale crater, Mars: A review after six Earth years of exploration with Curiosity. *Geochemistry* **80**, 125605 (2020).
44. G. M. Marion, D. C. Catling, J. S. Kargel, J. K. Crowley, Modeling calcium sulfate chemistries with applications to Mars. *Icarus* **278**, 31–37 (2016).
45. J. M. Keller, W. V. Boynton, S. Karunatillake, V. R. Baker, J. M. Dohm, L. G. Evans, M. J. Finch, B. C. Hahn, D. K. Hamara, D. M. Janes, K. E. Kerry, H. E. Newsom, R. C. Reedy, A. L. Sprague, S. W. Squyres, R. D. Starr, G. J. Taylor, R. M. S. Williams, Equatorial and midlatitude distribution of chlorine measured by Mars Odyssey GRS. *J. Geophys. Res. Planets* **111**, E03S08 (2006).
46. M. M. Osterloo, V. E. Hamilton, J. L. Bandfield, T. D. Glotch, A. M. Baldridge, P. R. Christensen, L. L. Tornabene, F. S. Anderson, Chloride-bearing materials in the southern highlands of Mars. *Science* **319**, 1651–1654 (2008).
47. M. M. Osterloo, F. S. Anderson, V. E. Hamilton, B. M. Hynek, Geologic context of proposed chloride-bearing materials on Mars. *J. Geophys. Res. Planets* **115**, E10012 (2010).
48. T. D. Glotch, J. L. Bandfield, M. J. Wolff, J. A. Arnold, C. Che, Constraints on the composition and particle size of chloride salt-bearing deposits on Mars. *J. Geophys. Res. Planets* **121**, 454–471 (2016).
49. T. D. Glotch, J. L. Bandfield, L. L. Tornabene, H. B. Jensen, F. P. Seelos, Distribution and formation of chlorides and phyllosilicates in Terra Sirenum, Mars. *Geophys. Res. Lett.* **37**, L16202 (2010).
50. M. H. Hecht, S. P. Kounaves, R. C. Quinn, S. J. West, S. M. M. Young, D. W. Ming, D. C. Catling, B. C. Clark, W. V. Boynton, J. Hoffmann, L. P. DeFlores, K. Gospodinova, J. Kapit, P. H. Smith, Detection of perchlorate and the soluble chemistry of martian soil at the Phoenix Lander site. *Science* **325**, 64–67 (2009).
51. S. P. Kounaves, M. H. Hecht, J. Kapit, K. Gospodinova, L. DeFlores, R. C. Quinn, W. V. Boynton, B. C. Clark, D. C. Catling, P. Hredzak, D. W. Ming, Q. Moore, J. Shusterman, S. Stroble, S. J. West, S. M. M. Young, Wet Chemistry experiments on the 2007 Phoenix Mars Scout Lander mission: Data analysis and results. *J. Geophys. Res. Planets* **115**, E00E10 (2010).
52. D. W. Ming, P. D. Archer Jr., D. P. Glavin, J. L. Eigenbrode, H. B. Franz, B. Sutter, A. E. Brunner, J. C. Stern, C. Freissinet, A. C. McAdam, P. R. Mahaffy, M. Cabane, P. Coll, J. L. Campbell, S. K. Atreya, P. B. Niles, J. F. Bell III, D. L. Bish, W. B. Brinckerhoff, A. Buch, P. G. Conrad, D. J. Des Marais, B. L. Ehlmann, A. G. Fairén, K. Farley, G. J. Flesch, P. Francois, R. Gellert, J. A. Grant, J. P. Grotzinger, S. Gupta, K. E. Herkenhoff, J. A. Hurowitz, L. A. Leshin, K. W. Lewis, S. M. McLennan, K. E. Miller, J. Moersch, R. V. Morris, R. Navarro-González, A. A. Pavlov, G. M. Perrett, I. Pradler, S. W. Squyres, R. E. Summons, A. Steele, E. M. Stolper, D. Y. Sumner, C. Szopa, S. Teinturier, M. G. Trainer, A. H. Treiman, D. T. Vaniman, A. R. Vasavada, C. R. Webster, J. J. Wray, R. A. Yingst; MSL Science Team, Volatile and organic compositions of sedimentary rocks in Yellowknife Bay, Gale Crater, Mars. *Science* **343**, 1245267 (2014).
53. M. Brundrett, W. Yan, M. C. Velazquez, B. Rao, W. A. Jackson, Abiotic reduction of chlorate by Fe(II) minerals: Implications for occurrence and transformation of oxy-chlorine species on Earth and Mars. *ACS Earth Space Chem.* **3**, 700–710 (2019).
54. M. Yeşilbaş, J.-F. Boily, Thin ice films at mineral surfaces. *J. Phys. Chem. Lett.* **7**, 2849–2855 (2016).
55. H. J. Lenferink, W. B. Durham, L. A. Stern, A. V. Pathare, Weakening of ice by magnesium perchlorate hydrate. *Icarus* **225**, 940–948 (2013).
56. G. M. Marion, D. C. Catling, K. J. Zahnle, M. W. Claire, Modeling aqueous perchlorate chemistries with applications to Mars. *Icarus* **207**, 675–685 (2010).
57. J. D. Toner, D. C. Catling, A low-temperature aqueous thermodynamic model for the Na–K–Ca–Mg–Cl–SO_4 system incorporating new experimental heat capacities in Na_2SO_4, K_2SO_4, and $MgSO_4$ solutions. *J. Chem. Eng. Data* **62**, 3151–3168 (2017).
58. J. D. Toner, D. C. Catling, B. Light, The formation of supercooled brines, viscous liquids, and low-temperature perchlorate glasses in aqueous solutions relevant to Mars. *Icarus* **233**, 36–47 (2014).
59. A. P. Zent, F. P. Fanale, Possible Mars brines: Equilibrium and kinetic considerations. *J. Geophys. Res. Solid Earth* **91**, 439–445 (1986).
60. F. Mees, T. V. Tursina, in *Interpretation of Micromorphological Features of Soils and Regoliths (Second Edition),* G. Stoops, V. Marcelino, F. Mees, Eds. (Elsevier, 2018), pp. 289–321.
61. T. Sievert, A. Wolter, N. B. Singh, Hydration of anhydrite of gypsum ($CaSO_4$.II) in a ball mill. *Cem. Concr. Res.* **35**, 623–630 (2005).
62. M. Vincendon, F. Forget, J. Mustard, Water ice at low to midlatitudes on Mars. *J. Geophys. Res. Planets* **115**, E10001 (2010).
63. L. Ojha, M. B. Wilhelm, S. L. Murchie, A. S. McEwen, J. J. Wray, J. Hanley, M. Massé, M. Chojnacki, Spectral evidence for hydrated salts in recurring slope lineae on Mars. *Nat. Geosci.* **8**, 829–832 (2015).
64. A. Wang, Z. Ling, Y. Yan, A. S. McEwen, M. T. Mellon, M. D. Smith, B. L. Jolliff, J. Head, Subsurface Cl-bearing salts as potential contributors to recurring slope lineae (RSL) on Mars. *Icarus* **333**, 464–480 (2019).
65. D. E. Stillman, T. I. Michaels, R. E. Grimm, K. P. Harrison, New observations of martian southern mid-latitude recurring slope lineae (RSL) imply formation by freshwater subsurface flows. *Icarus* **233**, 328–341 (2014).
66. M. F. Thomas, A. S. McEwen, C. M. Dundas, Present-day mass wasting in sulfate-rich sediments in the equatorial regions of Mars. *Icarus* **342**, 113566 (2020).
67. A. S. McEwen, E. Schafer, S. Sutton, M. Chojnacki, Remarkably widespread RSL activity following the Great Martian Dust Storm of 2018, in *EPSC-DPS Joint Meeting*, Geneva (The Europlanet Society, 2019), Abstract #557–552.
68. G. Munaretto, M. Pajola, G. Cremonese, C. Re, A. Lucchetti, E. Simioni, A. S. McEwen, A. Pommerol, P. Becerra, S. J. Conway, N. Thomas, M. Massironi, Implications for the origin and evolution of martian recurring slope lineae at Hale crater from CaSSIS observations. *Planet. Space Sci.* **187**, 104947 (2020).
69. R. V. Gough, D. L. Nuding, P. D. Archer Jr., M. S. Fernanders, S. D. Guzewich, M. A. Tolbert, A. D. Toigo, Changes in soil cohesion due to water vapor exchange: A proposed dry-flow trigger mechanism for recurring slope lineae on Mars. *Geophys. Res. Lett.* **47**, e2020GL087618 (2020).
70. D. T. Vaniman, S. J. Chipera, Transformations of Mg- and Ca-sulfate hydrates in Mars regolith. *Am. Mineral.* **91**, 1628–1642 (2006).
71. J. L. Bishop, A. Davila, J. Hanley, T. L. Roush, Dehydration-rehydration experiments with Cl salts mixed into Mars analog materials and the effects on their VNIR spectral properties, in *47th Lunar Planetary Science Conference*, The Woodlands, TX (Lunar and Planetary Institute, 2016), Abstract #1645.
72. M. Yeşilbaş, C. C. Lee, J.-F. Boily, Ice and cryosalt formation in saline microporous clay gels. *ACS Earth Space Chem.* **2**, 314–319 (2018).
73. J. Jaumot, R. Gargallo, A. de Juan, R. Tauler, A graphical user-friendly interface for MCR-ALS: A new tool for multivariate curve resolution in MATLAB. *Chemom. Intel. Lab. Syst.* **76**, 101–110 (2005).
74. J. D. Toner, D. C. Catling, R. S. Sletten, The geochemistry of Don Juan Pond: Evidence for a deep groundwater flow system in Wright Valley, Antarctica. *Earth Planet. Sci. Lett.* **474**, 190–197 (2017).
75. S. P. Kounaves, S. T. Stroble, R. M. Anderson, Q. Moore, D. C. Catling, S. Douglas, C. P. McKay, D. W. Ming, P. H. Smith, L. K. Tamppari, A. P. Zent, Discovery of natural perchlorate in the Antarctic Dry Valleys and its global implications. *Environ. Sci. Technol.* **44**, 2360–2364 (2010).
76. J. D. Toner, D. C. Catling, B. Light, A revised Pitzer model for low-temperature soluble salt assemblages at the Phoenix site, Mars. *Geochim. Cosmochim. Acta* **166**, 327–343 (2015).
77. J. L. Bishop, Reaction of Ca sulfates and chlorides in the martian near surface to create sinkholes and debris flows, in *GSA Annual Meeting*, Indianapolis, IN (Geological Society of America, 2018), Abstract #138–139.
78. T. L. Roush, J. F. Bell III, Thermal emission measurements 2000-400 cm^{-1}(5–25 μm) of Hawaiian palagonitic soils and their implications for Mars. *J. Geophys. Res. Planets* **100**, 5309–5317 (1995).
79. A. S. McEwen, L. Ojha, C. M. Dundas, S. S. Mattson, S. Byrne, J. J. Wray, S. C. Cull, S. L. Murchie, N. Thomas, V. C. Gulick, Seasonal flows on warm martian slopes. *Science* **333**, 740–743 (2011).
80. M. Yeşilbaş, J. L. Bishop, A molecular view of near surface brines on Mars through mid-infrared spectra of martian analogs mixed with Cl salts, in *51st Lunar Planetary Science Conference*, The Woodlands, TX (Lunar and Planetary Institute, 2020), Abstract #2788.
81. J. Hanley, J. B. Dalton III, V. F. Chevrier, C. S. Jamieson, R. S. Barrows, Reflectance spectra of hydrated chlorine salts: The effect of temperature with implications for Europa. *J. Geophys. Res. Planets* **119**, 2370–2377 (2014).
82. J. Hanley, V. F. Chevrier, R. S. Barrows, C. Swaffer, T. S. Altheide, Near- and mid-infrared reflectance spectra of hydrated oxychlorine salts with implications for Mars. *J. Geophys. Res.* **120**, 1415–1426 (2015).
83. J. L. Bishop, R. Quinn, M. D. Dyar, Spectral and thermal properties of perchlorate salts and implications for Mars. *Am. Miner.* **99**, 1580–1592 (2014).
84. L. Martinez-Uriarte, J. Dubessy, I. Bihannic, P. Boulet, P. Robert, Reference Raman spectra of $CaCl_2.nH_2O$ solids (n= 0, 2, 4, 6), in *11th International GeoRaman Conference*, St. Louis, Missourri (International GeoRaman Conference, 2014).
85. J. Hanley, D. J. Berget, V. F. Chevrier, Thermodynamic properties of aqueous chlorine oxyanion solutions and their applications to Mars, in *41st Lunar Planetary Science Conference*, The Woodlands, TX (Lunar and Planetary Institute, 2010), Abstract #1971.
86. D. E. Stillman, R. E. Grimm, Dielectric signatures of adsorbed and salty liquid water at the Phoenix landing site, Mars. *J. Geophys. Res. Planets* **116**, E09005 (2011).

87. J. Hanley, V. F. Chevrier, D. J. Berget, R. D. Adams, Chlorate salts and solutions on Mars. *Geophys. Res. Lett.* **39**, L08201 (2012).
88. J. D. Toner, D. C. Catling, B. Light, Soluble salts at the Phoenix Lander site, Mars: A reanalysis of the Wet Chemistry Laboratory data. *Geochim. Cosmochim. Acta* **136**, 142–168 (2014).
89. G. M. Marion, J. S. Kargel, *Cold Aqueous Planetary Geochemistry with FREZCHEM* (Springer, 2008), pp. 251.
90. R. V. Gough, V. F. Chevrier, M. A. Tolbert, Formation of liquid water at low temperatures via the deliquescence of calcium chloride: Implications for Antarctica and Mars. *Planet. Space Sci.* **131**, 79–87 (2016).
91. R. V. Gough, K. M. Primm, E. G. Rivera-Valentín, G. M. Martínez, M. A. Tolbert, Solid-solid hydration and dehydration of Mars-relevant chlorine salts: Implications for Gale Crater and RSL locations. *Icarus* **321**, 1–13 (2019).
92. R. V. Gough, V. F. Chevrier, K. J. Baustian, M. E. Wise, M. A. Tolbert, Laboratory studies of perchlorate phase transitions: Support for metastable aqueous perchlorate solutions on Mars. *Earth Planet. Sci. Lett.* **312**, 371–377 (2011).
93. D. L. Nuding, E. G. Rivera-Valentin, R. D. Davis, R. V. Gough, V. F. Chevrier, M. A. Tolbert, Deliquescence and efflorescence of calcium perchlorate: An investigation of stable aqueous solutions relevant to Mars. *Icarus* **243**, 420–428 (2014).
94. K. M. Primm, R. V. Gough, V. F. Chevrier, M. A. Tolbert, Freezing of perchlorate and chloride brines under Mars-relevant conditions. *Geochim. Cosmochim. Acta* **212**, 211–220 (2017).
95. A. F. Davila, I. Hawes, C. Ascaso, J. Wierzchos, Salt deliquescence drives photosynthesis in the hyperarid Atacama Desert. *Environ. Microbiol. Rep.* **5**, 583–587 (2013).
96. D. T. Vaniman, D. L. Bish, S. J. Chipera, C. I. Fialips, J. W. Carey, W. C. Feldman, Magnesium sulphate salts and the history of water on Mars. *Nature* **431**, 663–665 (2004).
97. R. Navarro-González, F. A. Rainey, P. Molina, D. R. Bagaley, B. J. Hollen, J. de la Rosa, A. M. Small, R. C. Quinn, F. J. Grunthaner, L. Cáceres, B. Gomez-Silva, C. P. McKay, Mars-like soils in the Atacama Desert, Chile, and the dry limit of microbial life. *Science* **302**, 1018–1021 (2003).
98. D. C. Catling, M. W. Claire, K. J. Zahnle, R. C. Quinn, B. C. Clark, M. H. Hecht, S. Kounaves, Atmospheric origins of perchlorate on Mars and in the Atacama. *J. Geophys. Res. Planets* **115**, E00E11 (2010).
99. J. Flahaut, M. Martinot, J. L. Bishop, G. R. Davies, N. J. Potts, Remote sensing and in situ mineralogic survey of the Chilean salars: An analog to Mars evaporate deposits? *Icarus* **282**, 152–173 (2017).
100. K. A. Warren-Rhodes, K. C. Lee, S. D. J. Archer, N. Cabrol, L. Ng-Boyle, D. Wettergreen, K. Zacny, S. B. Pointing; NASA Life in the Atacama Project Team, Subsurface microbial habitats in an extreme desert Mars-Analog Environment. *Front. Microbiol.* **10**, 69 (2019).
101. K. C. Benison, B. B. Bowen, Acid saline lake systems give clues about past environments and the search for life on Mars. *Icarus* **183**, 225–229 (2006).
102. B. B. Bowen, K. C. Benison, S. Story, Early diagenesis by modern acid brines in western Australia and implications for the history of sedimentary modification on Mars. *SEPM Spec. Publ.* **102**, 229–252 (2012).
103. M. Babel, B. C. Schreiber, Geochemistry of evaporites and evolution of seawater, in *Treatise on Geochemistry, 2nd Edition,* F. T. MacKenzie, Ed. (Elsevier, 2014), pp. 483–560.
104. J. L. Bishop, B. L. Anglen, L. M. Pratt, H. G. M. Edwards, D. J. Des Marais, P. T. Doran, A spectroscopy and isotope study of sediments from the Antarctic Dry Valleys as analogues for potential paleolakes on Mars. *Int. J. Astrobiol.* **2**, 273–287 (2003).
105. J. A. Mikucki, W. B. Lyons, I. Hawes, B. D. Lanoil, P. T. Doran, Saline lakes and ponds in the McMurdo Dry Valleys: Ecological analogs to martian paleolake environments, in *Life in Antarctic Deserts and Other Cold Dry Environments*, P. T. Doran, W. B. Lyons, D. M. McKnight, Eds. (Cambridge Univ. Press, 2010), pp. 160–194.
106. G. G. C. Claridge, The clay mineralogy and chemistry of some soils from the Ross Dependency, Antarctica. *N. Z. J. Geol. Geophys.* **8**, 186–220 (1965).
107. J. L. Bishop, H. B. Franz, W. Goetz, D. F. Blake, C. Freissinet, H. Steininger, F. Goesmann, W. B. Brinckerhoff, S. Getty, V. T. Pinnick, P. R. Mahaffy, M. D. Dyar, Coordinated analyses of Antarctic sediments as Mars analog materials using reflectance spectroscopy and current flight-like instruments for CheMin, SAM and MOMA. *Icarus* **224**, 309–325 (2013).
108. D. M. Anderson, Some thermodynamic relationships governing the behavior of permafrost and frozen ground, in *The Comparative Study of the Planets*, A. Coradini, M. Fulchignoni, Eds. (D. Reidel Publishing Company, 1982), pp. 435–440.
109. J. R. Keys, K. Williams, Origin of crystalline, cold desert salts in the McMurdo region, Antarctica. *Geochim. Cosmochim. Acta* **45**, 2299–2309 (1981).
110. M. Abelson, Y. Yechieli, O. Crouvi, G. Baer, D. Wachs, A. Bein, V. Shtivelman, Y. Enzel, A. Agnon, M. Stein, Evolution of the Dead Sea sinkholes, in *New Frontiers in Dead Sea Paleoenvironmental Research* (Geological Society of America, 2006), https://pubs.geoscienceworld.org/books/book/558/chapter/3802698/Evolution-of-the-Dead-Sea-sinkholes.
111. Y. Avni, N. Lensky, E. Dente, M. Shviro, R. Arav, I. Gavrieli, Y. Yechieli, M. Abelson, H. Lutzky, S. Filin, I. Haviv, G. Baer, Self-accelerated development of salt karst during flash floods along the Dead Sea Coast, Israel. *J. Geophys. Res. Earth* **121**, 17–38 (2016).
112. R. Naor, V. C. Gulick, Subsurface volume loss and collapse due to surface infiltration of Osuga Valles' catastrophic floods, Mars, in *EPSC-DPS Joint Meeting*, Geneva (The Europlanet Society, 2019), Abstract #1443–1442.
113. N. W. Hinman, N. A. Cabrol, V. Gulick, K. Warren-Rhodes, C. Tebes, G. Chong, C. Demergasso, Initial investigations of endoevaporitic gypsum habitats of Salar de Pajonales, Chile, in *Astrobiology Science Conference*, Mesa, AZ (Lunar and Planetary Institute, 2017), Abstract #3568.
114. D. J. Ward, J. M. Cesta, J. Galewsky, E. Sagredo, Late Pleistocene glaciations of the arid subtropical Andes and new results from the Chajnantor Plateau, northern Chile. *Quat. Sci. Rev.* **128**, 98–116 (2015).
115. Á. Kereszturi, Unique and potentially Mars-relevant flow regime and water sources at a high Andes-Atacama site. *Astrobiology* **20**, 723–740 (2020).
116. A. Klimchouk, *Hypogene Speleogenesis: Hydrogeological and Morphogenetic Perspective, NCKRI Special Paper 1* (National Cave and Karst Research Institute, 2007).
117. J. P. Galve, F. Gutiérrez, P. Lucha, J. Bonachea, J. Remondo, A. Cendrero, M. Gutiérrez, M. J. Gimeno, G. Pardo, J. A. Sánchez, Sinkholes in the salt-bearing evaporite karst of the Ebro River valley upstream of Zaragoza city (NE Spain): Geomorphological mapping and analysis as a basis for risk management. *Geomorphology* **108**, 145–158 (2009).
118. F. Gázquez, J.-M. Calaforra, P. Forti, J. De Waele, L. Sanna, The role of condensation in the evolution of dissolutional forms in gypsum caves: Study case in the karst of Sorbas (SE Spain). *Geomorphology* **229**, 100–111 (2015).
119. J. D. Martinez, K. S. Johnson, J. T. Neal, Sinkholes in evaporite rocks. *Am. Sci.* **86**, 38–51 (1998).
120. K. R. Moore, H. M. Holländer, M. Basri, M. Roemer, Application of geochemical and groundwater data to predict sinkhole formation in a gypsum formation in Manitoba, Canada. *Environ. Earth Sci.* **78**, 193 (2019).
121. P. Harris, J. von Holdt, S. Sebesta, T. Scullion, *Database of Sulfate Stabilization Projects in Texas* (Texas Transportation Institute, Texas A&M University, 2006).
122. Y. Farnam, S. Dick, A. Wiese, J. Davis, D. Bentz, J. Weiss, The influence of calcium chloride deicing salt on phase changes and damage development in cementitious materials. *Cem. Concr. Comp.* **64**, 1–15 (2015).
123. J. Raack, S. J. Conway, C. Herny, M. R. Balme, S. Carpy, M. R. Patel, Water induced sediment levitation enhances downslope transport on Mars. *Nat. Commun.* **8**, 1151 (2017).
124. C. Herny, S. J. Conway, J. Raack, S. Carpy, T. Colleu-Banse, M. R. Patel, Downslope sediment transport by boiling liquid water under Mars-like conditions: Experiments and potential implications for martian gullies. *Geol. Soc. Lond. Spec. Publ.* **467**, 373 (2018).
125. A. F. Davila, L. G. Duport, R. Melchiorri, J. Jänchen, S. Valea, A. de los Rios, A. G. Fairén, D. Möhlmann, C. P. McKay, C. Ascaso, J. Wierzchos, Hygroscopic salts and the potential for Life on Mars. *Astrobiology* **10**, 617–628 (2010).
126. A. S. McEwen, C. M. Dundas, S. S. Mattson, A. D. Toigo, L. Ojha, J. J. Wray, M. Chojnacki, S. Byrne, S. L. Murchie, N. Thomas, Recurring slope lineae in equatorial regions of Mars. *Nat. Geosci.* **7**, 53–58 (2014).
127. M. Chojnacki, A. McEwen, C. Dundas, L. Ojha, A. Urso, S. Sutton, Geologic context of recurring slope lineae in Melas and Coprates Chasmata, Mars. *J. Geophys. Res. Planets* **121**, 1204–1231 (2016).
128. J. Levy, Hydrological characteristics of recurrent slope lineae on Mars: Evidence for liquid flow through regolith and comparisons with Antarctic terrestrial analogs. *Icarus* **219**, 1–4 (2012).
129. E. I. Schaefer, A. S. McEwen, S. S. Sutton, A case study of recurring slope lineae (RSL) at Tivat crater: Implications for RSL origins. *Icarus* **317**, 621–648 (2019).
130. R. E. Grimm, K. P. Harrison, D. E. Stillman, Water budgets of martian recurring slope lineae. *Icarus* **233**, 316–327 (2014).
131. J. Heinz, D. Schulze-Makuch, S. P. Kounaves, Deliquescence-induced wetting and RSL-like darkening of a Mars analogue soil containing various perchlorate and chloride salts. *Geophys. Res. Lett.* **43**, 4880–4884 (2016).
132. V. F. Chevrier, E. G. Rivera-Valentin, Formation of recurring slope lineae by liquid brines on present-day Mars. *Geophys. Res. Lett.* **39**, L21202 (2012).
133. M. A. Kreslavsky, J. W. Head, Slope streaks on Mars: A new "wet" mechanism. *Icarus* **201**, 517–527 (2009).
134. J. L. Dickson, J. W. Head, J. S. Levy, D. R. Marchant, Don Juan Pond, Antarctica: Near-surface $CaCl_2$-brine feeding Earth's most saline lake and implications for Mars. *Sci. Rep.* **3**, 1166 (2013).
135. P. R. Christensen, B. M. Jakosky, H. H. Kieffer, M. C. Malin, H. Y. McSween Jr., K. Nealson, G. L. Mehall, S. H. Silverman, S. Ferry, M. Caplinger, M. Ravine, The Thermal Emission Imaging System (THEMIS) for the Mars 2001 Odyssey Mission. *Space Sci. Rev.* **110**, 85–130 (2004).
136. M. C. Malin, K. S. Edgett, Evidence for recent groundwater seepage and surface runoff on Mars. *Science* **288**, 2330–2335 (2000).
137. J. L. Heldmann, O. B. Toon, W. H. Pollard, M. T. Mellon, J. Pitlick, C. P. McKay, D. T. Andersen, Formation of martian gullies by the action of liquid water flowing

under current martian environmental conditions. *J. Geophys. Res. Planets* **110**, E05004 (2005).
138. S. J. Conway, M. R. Balme, A novel topographic parameterization scheme indicates that martian gullies display the signature of liquid water. *Earth Planet. Sci. Lett.* **454**, 36–45 (2016).
139. N. Hoffman, White Mars: A new model for Mars' surface and atmosphere based on CO_2. *Icarus* **146**, 326–342 (2000).
140. S. Diniega, C. J. Hansen, J. N. McElwaine, C. H. Hugenholtz, C. M. Dundas, A. S. McEwen, M. C. Bourke, A new dry hypothesis for the formation of martian linear gullies. *Icarus* **225**, 526–537 (2013).
141. C. M. Dundas, S. Diniega, A. S. McEwen, Long-term monitoring of martian gully formation and evolution with MRO/HiRISE. *Icarus* **251**, 244–263 (2015).
142. T. Kneissl, D. Reiss, S. van Gasselt, G. Neukum, Distribution and orientation of northern-hemisphere gullies on Mars from the evaluation of HRSC and MOC-NA data. *Earth Planet. Sci. Lett.* **294**, 357–367 (2010).
143. T. de Haas, D. Ventra, E. Hauber, S. J. Conway, M. G. Kleinhans, Sedimentological analyses of martian gullies: The subsurface as the key to the surface. *Icarus* **258**, 92–108 (2015).
144. K. S. Auld, J. C. Dixon, A classification of martian gullies from HiRISE imagery. *Planet. Space Sci.* **131**, 88–101 (2016).
145. V. C. Gulick, N. Glines, Gully Formation on Mars: Implications for Late Paleo Microclimates, in *Late Mars Workshop*, Houston, TX (Lunar and Planetary Institute, 2018), Abstract #5028.
146. G. Jouannic, J. Gargani, S. J. Conway, F. Costard, M. R. Balme, M. R. Patel, M. Massé, C. Marmo, V. Jomelli, G. G. Ori, Laboratory simulation of debris flows over sand dunes: Insights into gully-formation (Mars). *Geomorphology* **231**, 101–115 (2015).
147. W. C. Feldman, T. H. Prettyman, S. Maurice, S. Nelli, R. Elphic, H. O. Funsten, O. Gasnault, D. J. Lawrence, J. R. Murphy, R. L. Tokar, D. T. Vaniman, Topographic control of hydrogen deposits at low latitudes to midlatitudes of Mars. *J. Geophys. Res. Planets* **110**, E11009 (2005).
148. B. M. Jakosky, M. T. Mellon, E. S. Varnes, W. C. Feldman, W. V. Boynton, R. M. Haberle, Mars low-latitude neutron distribution: Possible remnant near-surface water ice and a mechanism for its recent emplacement. *Icarus* **175**, 58–67 (2005).
149. M. T. Mellon, B. M. Jakosky, The distribution and behavior of martian ground ice during past and present epochs. *J. Geophys. Res. Planets* **100**, 11781–11799 (1995).
150. M. T. Mellon, B. M. Jakosky, S. E. Postawko, The persistence of equatorial ground ice on Mars. *J. Geophys. Res. Planets* **102**, 19357–19369 (1997).
151. J. L. Bandfield, W. C. Feldman, Martian high latitude permafrost depth and surface cover thermal inertia distributions. *J. Geophys. Res. Planets* **113**, E08001 (2008).
152. S. J. Conway, M. R. Balme, Decameter thick remnant glacial ice deposits on Mars. *Geophys. Res. Lett.* **41**, 5402–5409 (2014).
153. J. J. Plaut, A. Safaeinili, J. W. Holt, R. J. Phillips, J. W. Head III, R. Seu, N. E. Putzig, A. Frigeri, Radar evidence for ice in lobate debris aprons in the mid-northern latitudes of Mars. *Geophys. Res. Lett.* **36**, L02203 (2009).
154. W. V. Boynton, W. C. Feldman, S. W. Squyres, T. H. Prettyman, J. Bruckner, L. G. Evans, R. C. Reedy, R. Starr, J. R. Arnold, D. M. Drake, P. A. J. Englert, A. E. Metzger, I. Mitrofanov, J. I. Trombka, C. d'Uston, H. Wänke, O. Gasnault, D. K. Hamara, D. M. Janes, R. L. Marcialis, S. Maurice, I. Mikheeva, G. J. Taylor, R. Tokar, C. Shinohara, Distribution of hydrogen in the Near Surface of Mars: Evidence for subsurface ice deposits. *Science* **297**, 81–85 (2002).
155. M. Vincendon, J. Mustard, F. Forget, M. Kreslavsky, A. Spiga, S. Murchie, J.-P. Bibring, Near-tropical subsurface ice on Mars. *Geophys. Res. Lett.* **37**, L01202 (2010).
156. R. Orosei, S. E. Lauro, E. Pettinelli, A. Cicchetti, M. Coradini, B. Cosciotti, F. Di Paolo, E. Flamini, E. Mattei, M. Pajola, F. Soldovieri, M. Cartacci, F. Cassenti, A. Frigeri, S. Giuppi, R. Martufi, A. Masdea, G. Mitri, C. Nenna, R. Noschese, M. Restano, R. Seu, Radar evidence of subglacial liquid water on Mars. *Science* **361**, 490–493 (2018).
157. Y. Chen, Y. Liu, Y. Guan, J. M. Eiler, C. Ma, G. R. Rossman, L. A. Taylor, Evidence in Tissint for recent subsurface water on Mars. *Earth Planet. Sci. Lett.* **425**, 55–63 (2015).
158. C. McKay, D. Andersen, W. Pollard, J. Heldmann, P. Doran, C. Fritsen, J. Priscu, in *Water on Mars and Life*, T. Tokano, Ed. (Springer-Verlag, 2005), pp. 219–233.
159. N. Cuozzo, R. S. Sletten, Y. Hu, L. Liu, F.-Z. Teng, B. Hagedorn, Silicate weathering in antarctic ice-rich permafrost: Insights using magnesium isotopes. *Geochim. Cosmochim. Acta* **278**, 244–260 (2020).

Acknowledgments: We are grateful for the use of the cryo-FTIR laboratory facilities of J.-F. Boily (Department of Chemistry, Umeå University), to the HiRISE team for collecting the images used in this study, to T. Roush for providing the Mauna Kea ash sample, to M. Gruendler for preparing the sample video, and to V. Robles Bravo for sharing his image of gypsum beds at Salar de Pajonales. We also wish to thank L. Gruendler for editorial assistance, R. Klima for handling the review of our paper, and E. Rampe and an anonymous reviewer for helpful comments that improved the manuscript. **Funding:** Support from the NASA Astrobiology Institute (NAI) grant number NNX15BB01 to J.L.B., M.Y., N.W.H., Z.F.M.B., and V.C.G. is much appreciated. M.Y. is grateful for support from the NASA Postdoctoral Program (NPP) within the NAI that is administered by the Universities Space Research Association (USRA) under contract with NASA. M.Y. also thanks the Swedish Research Council grant (2018-06694) for support. Z.F.M.B. thanks the Clay Minerals Society and the Geological Society of America for support. **Author contributions:** J.L.B. conceived of this study, prepared the samples and data, and led assembly of the manuscript text and figures. M.Y. performed the low-temperature spectroscopy studies, analyzed the data, and provided experience on thin films of water on mineral surfaces. N.W.H. contributed to the chemical analyses of sulfates and Cl salts. Z.F.M.B. characterized and analyzed the spectral properties and chemistry of samples from a soil pit in the MDV. P.A.J.E. characterized and analyzed numerous Antarctic soils and sediments to provide an understanding of chemical trends in the MDV. J.D.T. modeled the solubility of gypsum in the presence of Cl salts and contributed experience from the MDV field sites. A.S.M. provided insights and context on martian RSL. V.C.G. provided insights and context on martian gullies and RSL. E.K.G. collected the Antarctic samples and provided context on the field sites. C.K. contributed elemental abundances of the Antarctic samples. All authors participated in the manuscript assembly. **Competing interests:** The authors declare that they have no competing interests. **Data and materials availability:** All data needed to evaluate the conclusions in this paper are present in the paper and/or the Supplementary Materials. The low-temperature ATR data are included in the external data file S1. Additional data related to this paper may be requested from the authors.

Submitted 21 August 2020
Accepted 15 December 2020
Published 3 February 2021
10.1126/sciadv.abe4459

Citation: J. L. Bishop, M. Yeşilbaş, N. W. Hinman, Z. F. M. Burton, P. A. J. Englert, J. D. Toner, A. S. McEwen, V. C. Gulick, E. K. Gibson, C. Koeberl, Martian subsurface cryosalt expansion and collapse as trigger for landslides. *Sci. Adv.* **7**, eabe4459 (2021).

Martian subsurface cryosalt expansion and collapse as trigger for landslides

J. L. Bishop, M. Yesilbas, N. W. Hinman, Z. F. M. Burton, P. A. J. Englert, J. D. Toner, A. S. McEwen, V. C. Gulick, E. K. Gibson and C. Koeberl

Sci Adv **7** (6), eabe4459.
DOI: 10.1126/sciadv.abe4459